

**Preliminary Report
of
the Hakuho Maru Cruise KH-94-1**

February 24 - March 22, 1994

Reproduction and recruitment of small pelagic fishes
in the Kuroshio system

Ocean Research Institute
University of Tokyo
1997

**Preliminary Report
of
the Hakuho Maru Cruise KH-94-1**

February 24 - March 22, 1994

Reproduction and recruitment of small pelagic fishes
in the Kuroshio system

By
The Scientific Members of the Expedition
Edited by
Ichiro AOKI

Contents

1. Introduction (I.Aoki)	1
2. Scientists Aboard	3
3. Track charts of the Cruise KH-94-1 (C.Igarashi)	4
4. Drift Charts of the Cruise KH-94-1 (C.Igarashi)	6
5. Outline of Scientific Results	8
5.1 Observation of water temperature and salinity along the Kuroshio Current (T.Inagaki, C.Igarashi, T.Komatsu)	8
5.2 Reproductive ecology of Japanese sardine <i>Sardinops melanostictus</i> and chub mackerel <i>Scomber japonicus</i> (I.Aoki, M.Shiraishi, T.Yamada, T.Komatsu, K.Hwang)	14
5.3 Distribution of plankton and micronecton by acoustic remote-sensing (T.Inagaki, K.Miyashita)	19
5.4 Seawater sampling for elements-analysis using ICP-spectrometer (M.Shiraishi)	20
5.5 Spawning frequency and batch fecundity of the Japanese anchovy <i>Engraulis japonicus</i> caught at the nearshore of Miyake Island (Y.Tsuruta, H.Niwa)	22
5.6 Physical and biological fine structure in the Enshu-nada Sea (S.Kimura, H.Nakata, T.Sugimoto)	25
5.7 Estimation of volume, heat and salt transports across the Kuroshio off Cape Ashizuri (H.Ichikawa, N.Gohda, T.Tamura, T.Fujimoto)	30
5.8 Aerosol particle concentration over the south ocean of Japan Islands in winter (K.Miura, H.Kojima, K.Matsuda, M.Hidaka, S.Nakae)	36
6. Stations and working log (C.Igarashi)	41

Introduction

Three pelagic fish populations of sardine, anchovy and mackerel show long-term fluctuations in different phase. The dominant fish was anchovy in the 1960s, mackerel in the 1970s, and sardine in the 1980s. The 1990s is an age when changes are coming in the pelagic fish community. Sardine populations continue to decline, and anchovy appear to enter a period of increase. Though the mackerel stock remain at a extremely low level, survival of young-of-the year mackerel is not entirely bad in the recent years. Thus, it is important for an insight into trends in the three pelagic fish populations to investigate their spawning and survival of eggs and larvae in these years.

Off the Pacific coast of Japan, reproductive processes in these pelagic fishes contain a common feature of being under the influence of the Kuroshio. The locations and seasons of their spawning are partly different with overlapping. The three fish species spawn small separate floating eggs in several batches, but the numbers of spawning times, spawning frequencies and fecundity in a spawning season are probably different. The difference in the spawning patterns may lead to that in the subsequent transport and survival of eggs and larvae by being coupled with oceanic environments.

The objectives of the Hakuho Maru KH-94-1 Cruise were to study the mechanisms of reproductions and recruitment of the small pelagic fishes in relation to physical oceanographic environments. A total of 33 scientists with various specialties from 7 institutions participated. At present, when the spawning grounds of sardine off southern Kyushu have disappeared, these survey areas cover a great part of spawning areas of the three pelagic fishes off the Pacific coast of Japan.

To estimate abundance, distribution and spawning activity of fish, acoustic surveys and gill net samplings were carried out in Tosa Bay and area around Izu Islands. A lot of fish samples were collected, and it is worth special mention to have taken many anchovy with hydrated eggs around Miyake-jima adjacent to the Kuroshio. To examine relationship between survival of transported larvae and physical environments, eggs and larvae were collected with environmental measurements at many stations in Kumano-nada and Enshu-nada. Several Argos buoys were released in eastern Tosa Bay where a great many eggs occurred and in the Kuroshio off Cape Ashizuri. A ADCP was moored off Oshima to measure current and zooplankton acoustically. In addition, flow volume, heat and salt transports were measured along a transect across the Kuroshio off Cape Ashizuri. Observation of aerosol particle concentrations in the air was also conducted along track lines of this cruise.

On behalf of all scientists aboard, I express our sincere thanks to Captain Hideji Shimamune and all the crew of the R.V. Hakuho Maru for their hearty help and support throughout the cruise in spite of around-the-clock operation. This was the last Hakuho Maru cruise of Captain Hideji Shimamune. We wish to thank you again for his efforts and support for a long time. Ms. Fukuko Sogo, ORI greatly help us in editing this report.

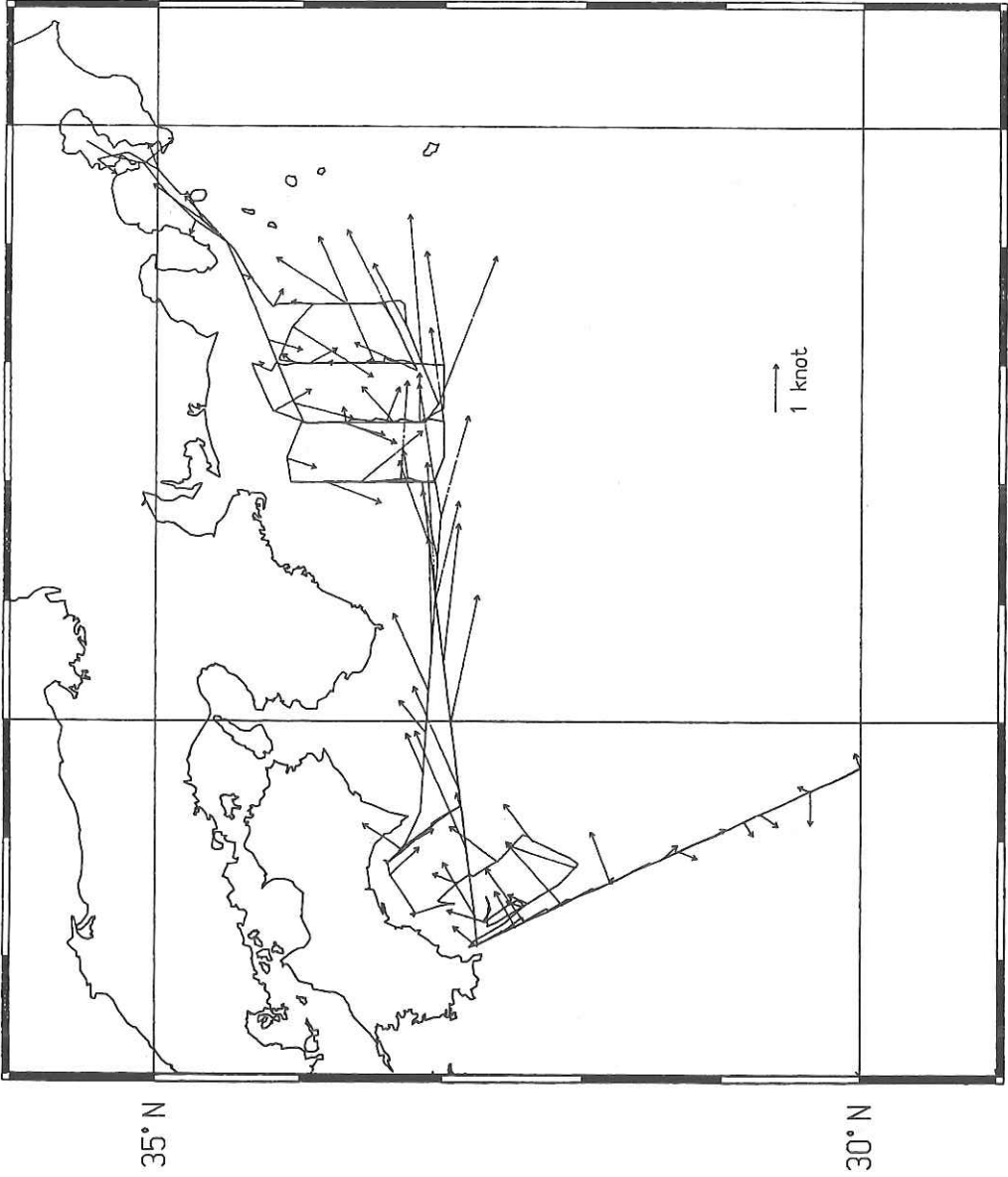
Ichiro Aoki
Chief Scientist

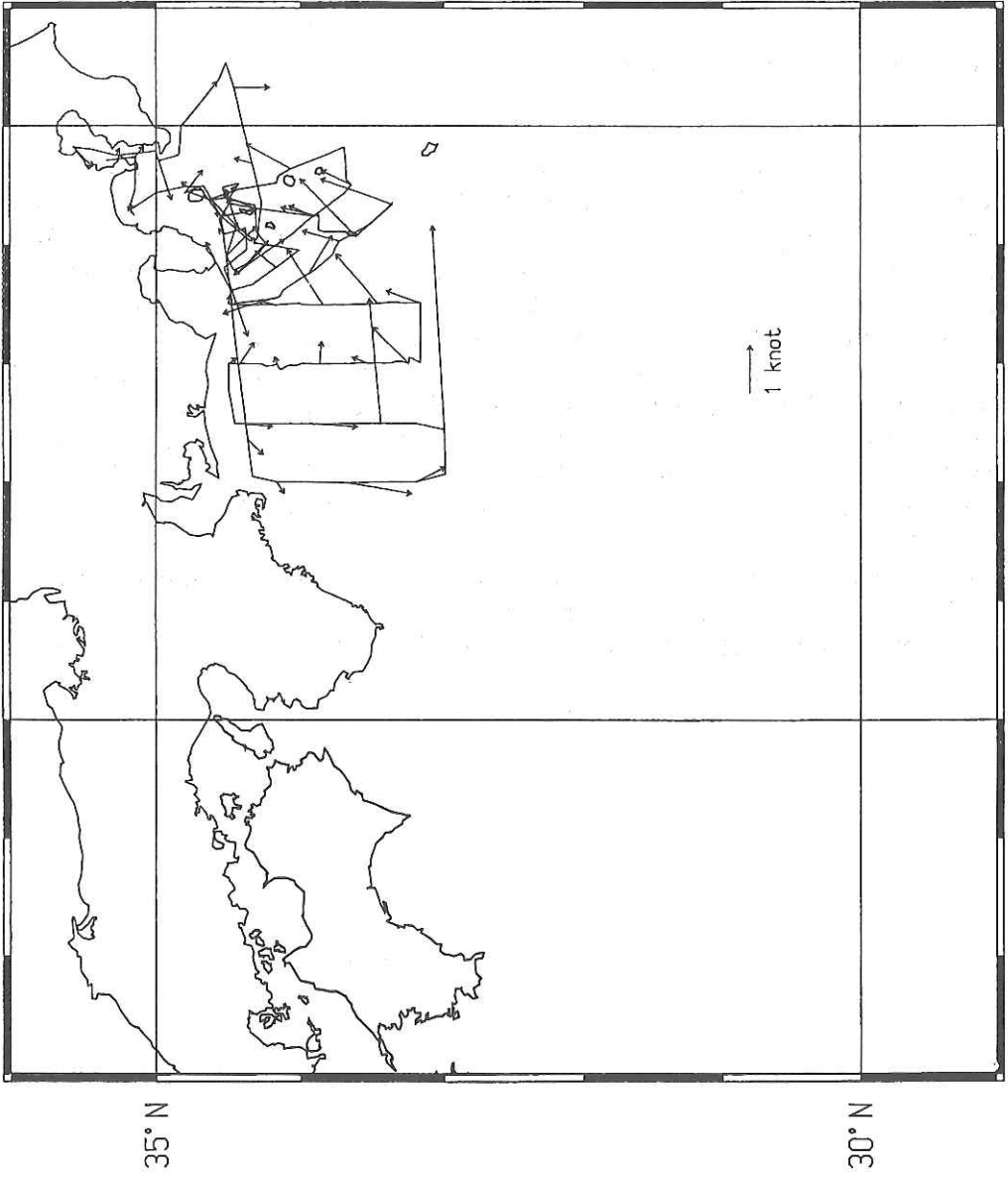


List of the scientists aboard

Aoki,	Ichiro:	Chief Scientist, Ocean Research Institute, University of Tokyo
Sugimoto,	Takashige:	Ocean Research Institute, University of Tokyo
Nakata,	Hideaki:	Ocean Research Institute, University of Tokyo
Komatsu,	Teruhisa:	Ocean Research Institute, University of Tokyo
Ishida,	Kennich:	Ocean Research Institute, University of Tokyo
Kishi,	Michio:	Ocean Research Institute, University of Tokyo
Kimura,	Shingo:	Ocean Research Institute, University of Tokyo
Igarashi,	Chiaki:	Ocean Research Institute, University of Tokyo
Inagaki,	Tadashi:	Ocean Research Institute, University of Tokyo
Nagae,	Hideo:	Ocean Research Institute, University of Tokyo
Hwang,	Kangseok:	Ocean Research Institute, University of Tokyo
Kawser,	Ahmed:	Ocean Research Institute, University of Tokyo
Azuma,	Nobuyuki:	Ocean Research Institute, University of Tokyo
Miyashita,	Kazushi:	Ocean Research Institute, University of Tokyo
Yamada,	Tomohide:	Ocean Research Institute, University of Tokyo
Kasai,	Akihide:	Ocean Research Institute, University of Tokyo
Koizumi,	Noriyuki:	Ocean Research Institute, University of Tokyo
Tadokoro,	Kazuaki:	Ocean Research Institute, University of Tokyo
Nakai,	Munenori:	Ocean Research Institute, University of Tokyo
Furushima,	Yasuo:	Ocean Research Institute, University of Tokyo
Sainz-Trápaga,	Susana:	Ocean Research Institute, University of Tokyo
Himi,	Machiko:	Tokyo University of Fisheries
Gohda,	Noriaki:	Faculty of Engineering, Hiroshima University
Tamura,	Tadashi:	Graduate School of Engineering, Hiroshima University
Fujimoto,	Teruaki:	Graduate School of Engineering, Hiroshima University
Ichikawa,	Hiroshi:	Faculty of Fisheries, Kagoshima University
Kojima,	Hiroshi:	Faculty of Science and Technology , Science University of Tokyo
Hidaka,	Makiko:	Faculty of Science, Science University of Tokyo
Matsuda,	Kazuhide:	Faculty of Science, Science University of Tokyo
Shiraishi,	Manabu:	National Research Institute of Aquaculture
Tsuruta,	Yoshinari:	Hokkaido National Fisheries Research Institute
Niwa,	Hirosato:	National Research Institute of Fisheries Engineering

DRIFT CHART





Observation of water temperature and salinity along the Kuroshio Current

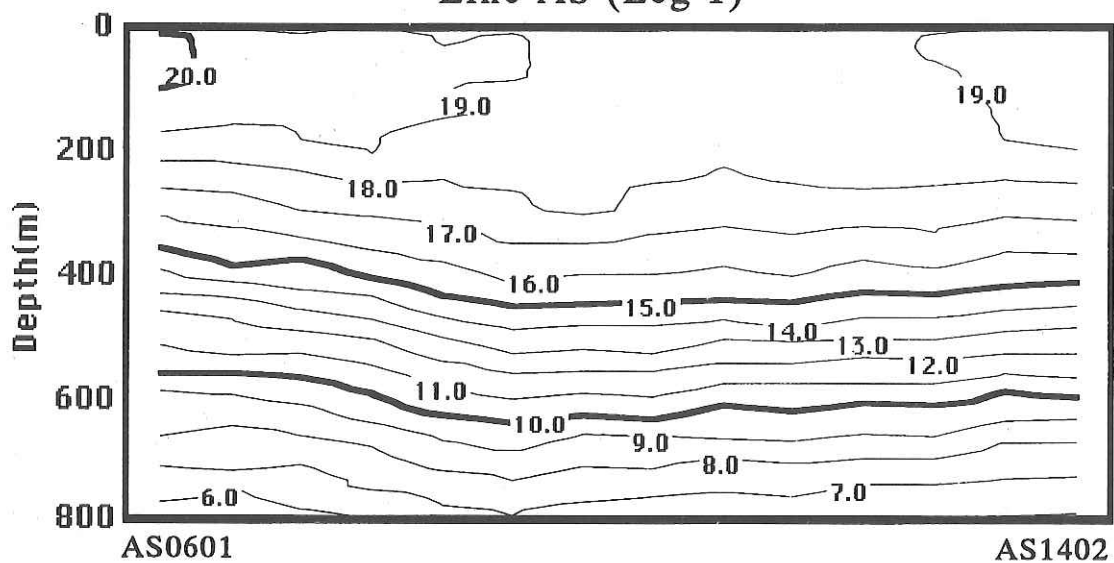
T. Inagaki, C. Igarashi, and K. Komatsu

Ocean Research Institute, University of Tokyo

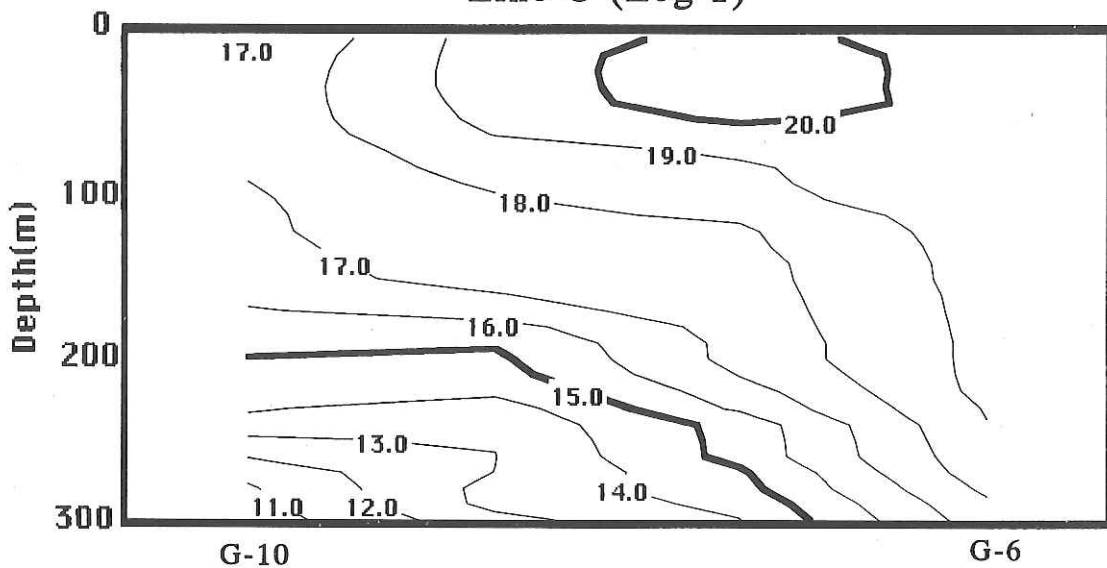
Water temperature and salinity distributions probably influence spawning ground formation of pelagic fish and growth and development of larval fish. These parameters indicate positions of the Kuroshio Current, which relates to transports of eggs and larvae of pelagic fish. The observations of water temperature and salinity were made by CTD (SEABIRD) or XBT casting. Unfortunately, the conductivity sensor did not work well in the cruise. Thus, only the vertical profiles of water temperature were drawn along the following transect lines: Line AS from Stns. AS0601 to AS1402, Line G from Stns. G-10 to G-6, Line KX from Stns. KX-1 to KX-8 and Line K from Stns. K-38 to K-34 in Leg. 1 and Line G from Stns. G-26 to G-30, Line G from Stns. G-12 to G-25, Line K from Stn. K-86 to K-78, Line K from K-56 to K-48 and Line KS from Stns. KS-2 to KS-8 in Leg. 2. Line KX and Line KS are based on the data from XBT and the other lines are on the data from CTD.

The Kuroshio Current approached the Ashizuri Peninsula off the Shikoku Island (Line AS and Line G) and situated around Stn. KX-8 off the Enshu-Nada in Leg. 1. In Leg. 2, the Kuroshio Current washed the Izu Islands (Line G from Stns. G-26 to G-30 and that from Stn. G-12 to G-25).

Line AS (Leg 1)

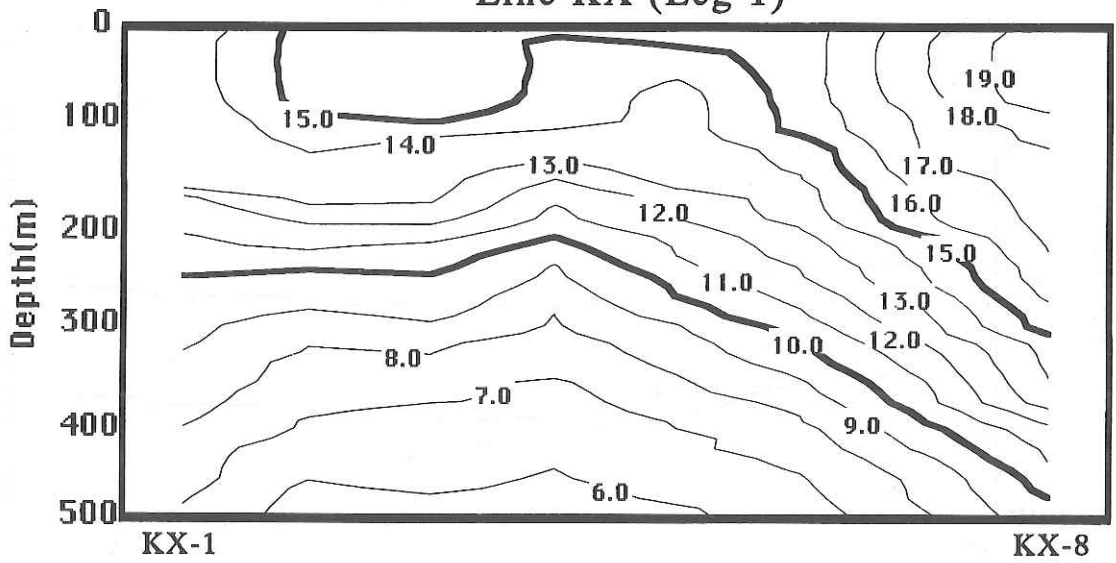


Line G (Leg 1)

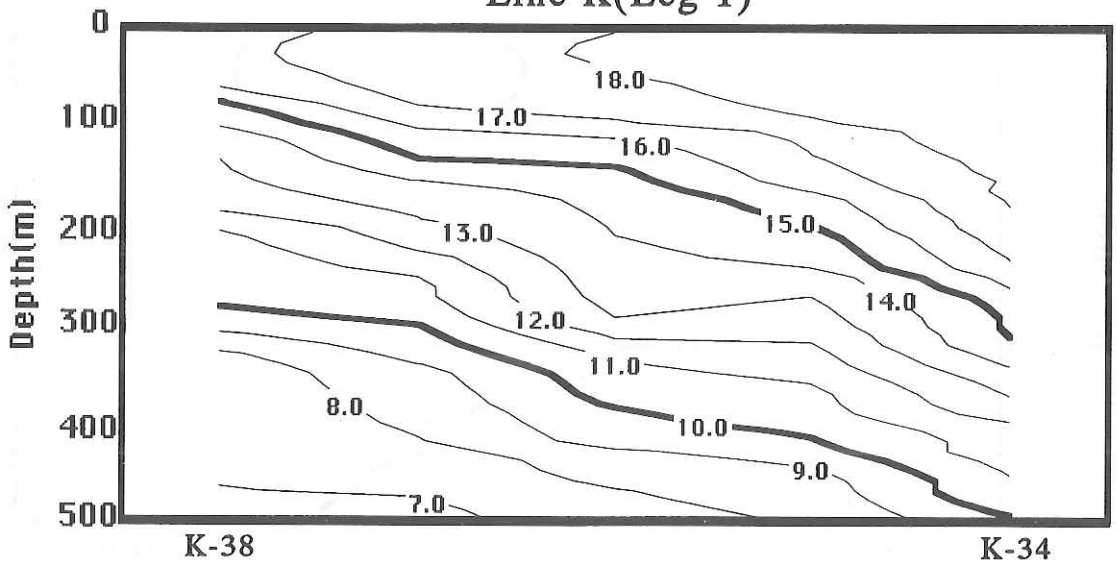


Temperature section along Line AS and Line G (Leg 1)

Line KX (Leg 1)

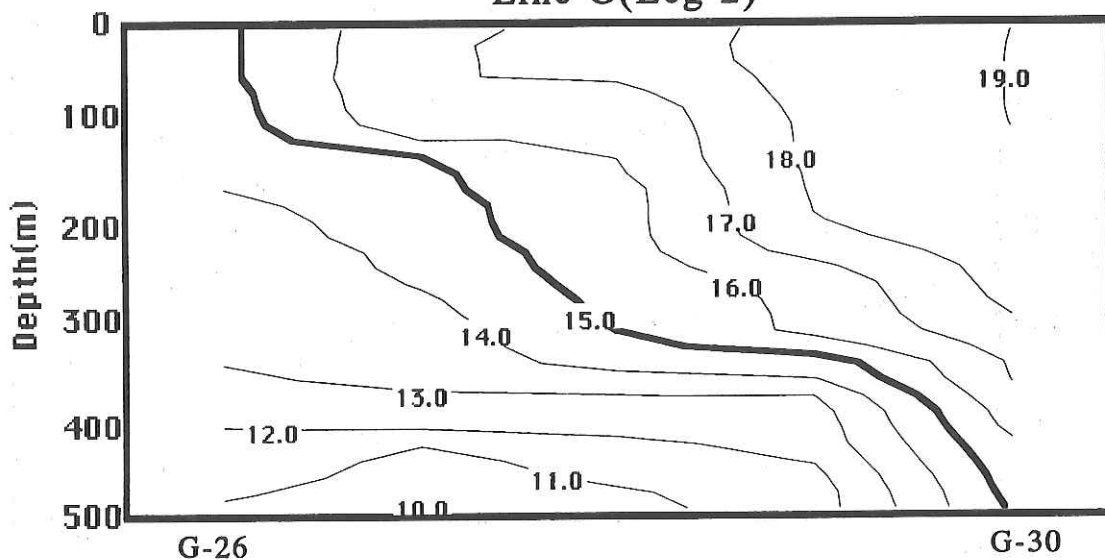


Line K (Leg 1)

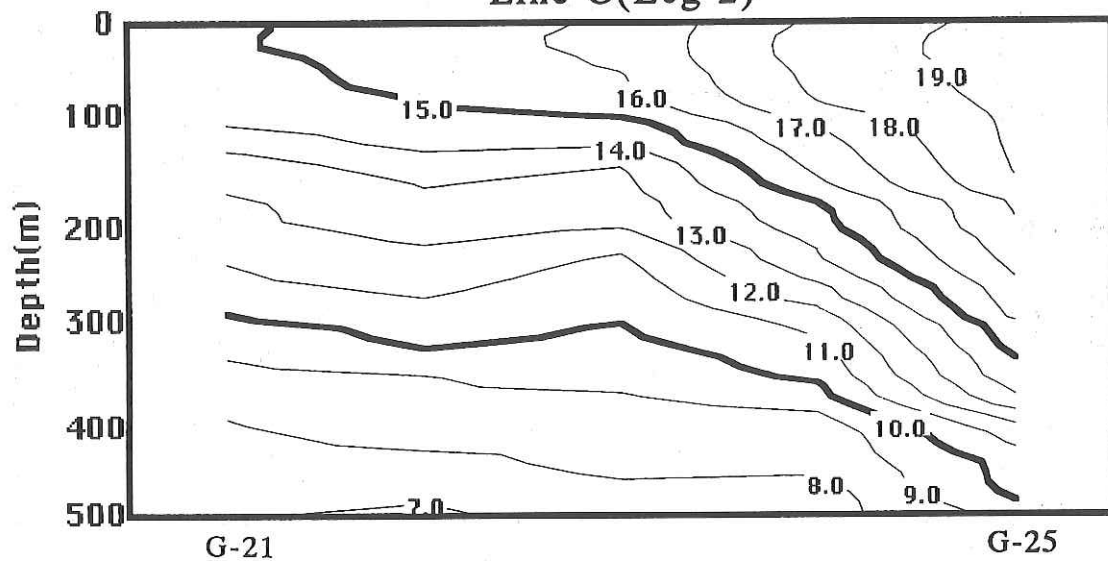


Temperature section along Line KX and K (Leg 1)

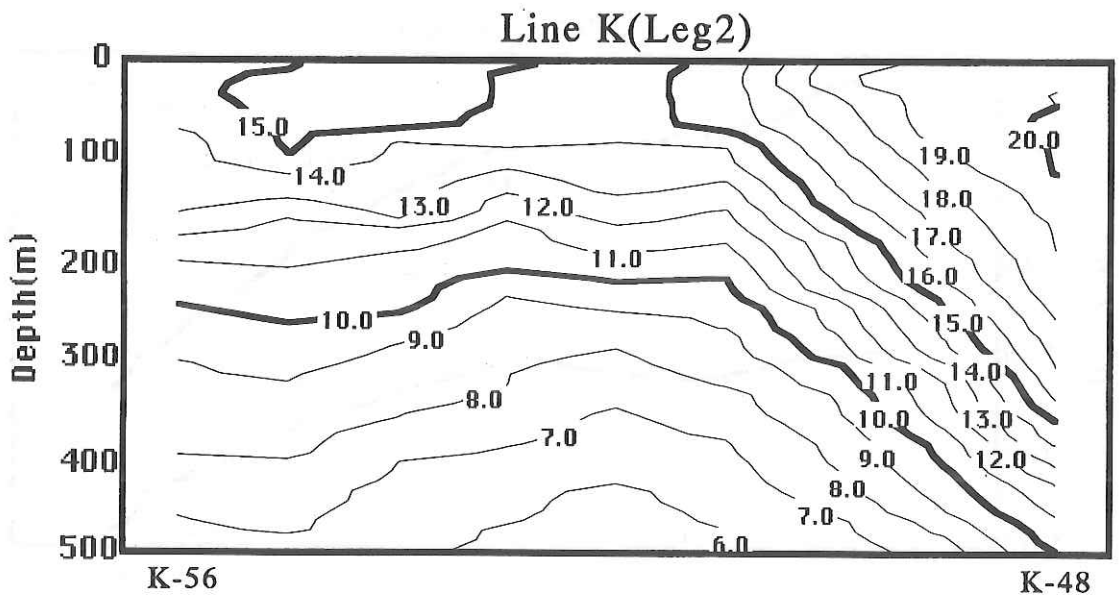
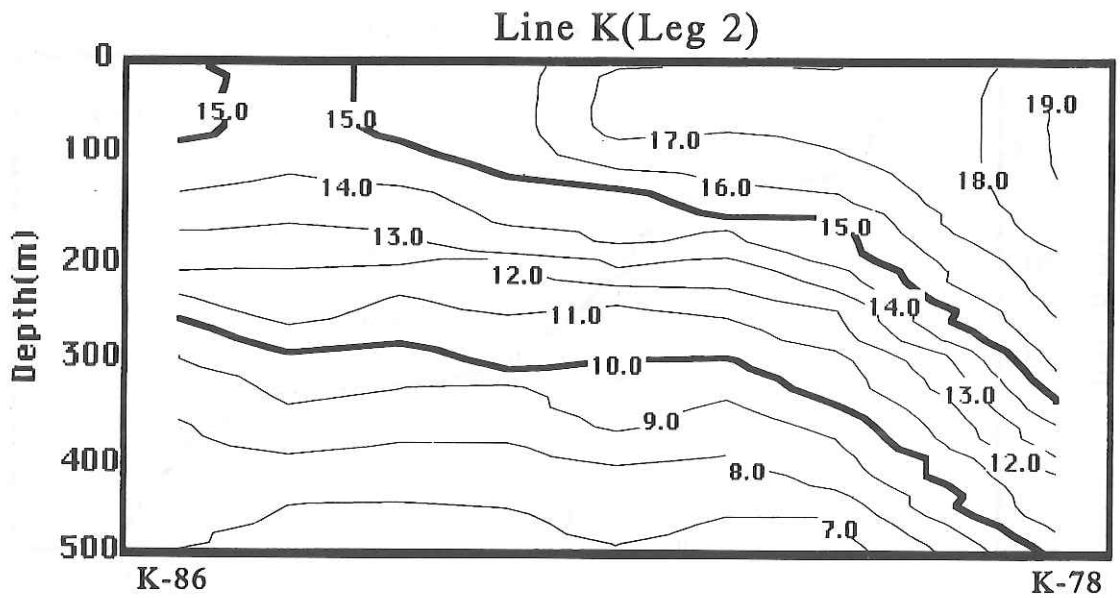
Line G(Leg 2)



Line G(Leg 2)

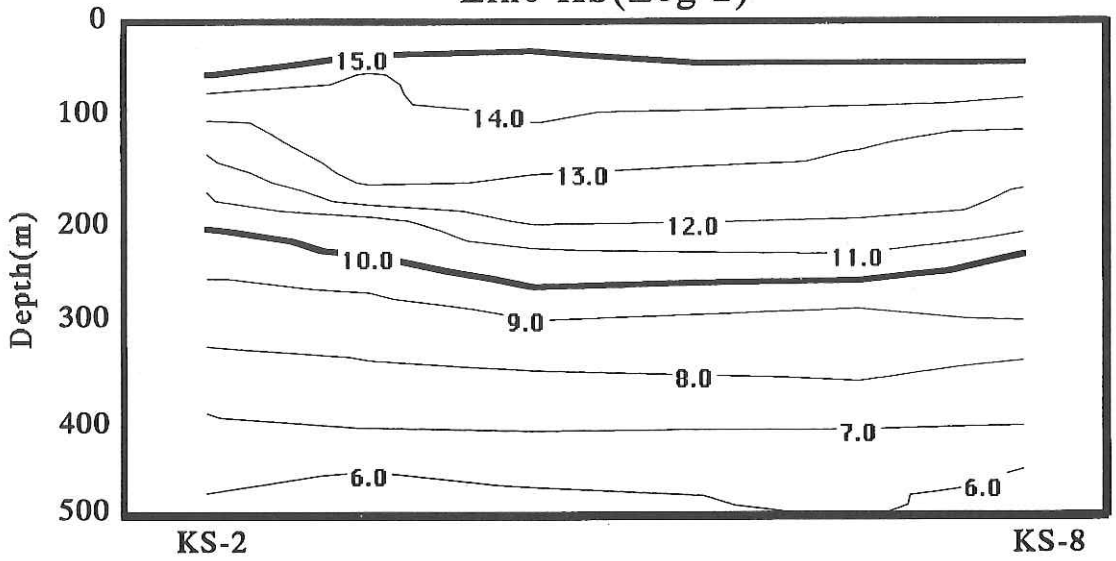


Temperature section along Line G (Leg 2)



Temperature section along Kine K (Leg 2)

Line KS(Leg 2)



Temperature section along Line KS (Leg 2)

Reproductive ecology of Japanese sardine *Sardinops melanostictus* and chub mackerel *Scomber japonicus*

Ichiro Aoki¹, Manabu Shiraishi², Tomohide Yamada¹, Teruhisa Komatsu¹, and Kangseok Hwang¹

¹Ocean Research Institute, University of Tokyo

²National Research Institute of Aquaculture

Introduction

Spawning pattern is a fundamental element in understanding fish-stock variability in the context of life-history strategies in which individuals reproduce. It has been known that during periods of high abundance, the spawning grounds of the Japanese sardine mainly occur in the area around southern Kyushu, southwestern Japan. At present, spawning sardine do not appear off southern Kyushu, but their main spawning grounds are in Tosa Bay and around Izu Islands. Especially, the area around Izu Islands is also the main spawning grounds of chub mackerel and anchovy.

This study investigated distribution and spawning pattern of sardine and mackerel in relation to water temperature, chlorophyll and zooplankton distributions in the spawning grounds.

Methods

The surveys consisted of grid surveys with wide areal coverage in Tosa Bay and around Izu Islands. Acoustic observations were made with 50kHz echo sounder, a Furuno FQ71, mounted on the RV 'Hakuho Maru' to quantify fish and zooplankton. The acoustic system processed echoes and output the mean volume backscattering strength (SV in dB) in real time for nine 10 m depth strata from 10 to 100m at horizontal integration intervals of 0.5 nautical miles (nm). Each 0.5 nm × 10 m segment was classified by observing echograms: one (fish echo) where echotraces of pelagic schooling fish occurred, and the other (plankton echo) where only weak diffuse scattering layers due to plankton appeared.

Surface temperature, salinity and chl-a concentration were measured along tracklines throughout the surveys. CTD and XBT casts were also made to determine oceanographic structure in the survey area. Sardine and mackerel were sampled with gill nets and fishing lines. The scaled body length and body weight of collected fish were measured and used for calculations of target strength and biomass. Maturity data were also obtained from the samples.

Results and Discussion

(1) *Distribution of chl-a concentration*

Chl-a distribution is illustrated in Fig. 1, and SST is shown in Fig. 2. At the time of the survey, the Kuroshio flowed northeastward south of Miyake-jima Island. The chl-a

concentration was relatively high more than $1.5 \mu\text{g/l}$ as a whole including the Kuroshio waters. High concentration areas occurred around Nii-jima Island and Zeni-su shoal and off Suruga Bay.

(2) *Distribution of zooplankton abundance*

Fig. 2 shows SST and 5 nm mean SV excluding fish echoes for 10-50 m depth which indicates zooplankton abundance. The zooplankton biomass were distributed in accordance with the SST and Kuroshio current; it was high in the waters $< 17^\circ\text{C}$ and low in the offshore high-temperature Kuroshio region. The zooplankton abundance varied inversely with water temperature as it was higher in the small cold water mass south of Kozu-shima Island than in the surrounding waters (Fig. 3).

(3) *Distribution of pelagic fish schools*

Fish schools occurred mostly in the 20-50 m depth, and fish sampling indicated that most of them were sardine. Anchovy also coexisted, but it is very difficult to discriminate the two fish species by echotraces. Fish schools which occurred in the depth > 50 m were probably chub mackerel and/or jack mackerel and less than in the upper layer.

Fig. 4 shows 5 nm mean SV from fish echoes in the 10-50 m depth. Fish schools were concentrated in the coastal side of the line drawn between Omurodashi and Zenisu shoals where SST $< 16^\circ\text{C}$ except for the area around Miyake-jima Island. The concentration area corresponded with the area of high chl-a and zooplankton abundance. Mean area backscattering strengths of the survey area were -56.4 dB for the 10-50m depth and -61.8 dB for the 50 - 100 m depth. Given that all fish echoes in the 10-50m depth were due to sardine, fish abundance was calculated to be 47,000 ton.

(4) *Spawning of sardine*

For histological observations of ovaries, paraffin sections of ovary portions were prepared, stained by HE, and checked for the presence of postovulatory follicles.

The time needed for the disappearance of the postovulatory follicles of Japanese sardine varies depending on the water temperature. It was experimentally confirmed that when the water temperature is 17°C the postovulatory follicles have disappeared from the ovary within 48 hours after spawning. We studied the spawning of Japanese sardine in 1994 utilizing this phenomenon.

The average GSI of females in the sea area around the Izu Islands was 7.75 in March. There was little difference in the percentage of females participating in spawning between females of body length < 18 cm (about 70%) and those of body length ≥ 18 cm (about 60%) (Fig. 5). Also, the condition factor of females of body lengths < 18 cm was high (Fig. 6).

There was difference in GSI between females sampled at three station in Tosa Bay (Fig. 7), though more females from Station 1 had postovulatory follicles than did those from other stations. We thus assumed that spawning was actively occurring at Station 1 (Fig. 8). There exists little information, however, on the Japanese sardine spawning cycle, so further detailed study is needed.

Condition factor of the spawning sardine in 1994 was high. The age at which these sardine started spawning was earlier than that in the high abundance period. From these facts we have conjectured that because of the decreased size of Japanese sardine stock, the amount of feed ingested per individual increased, and the nutritive conditions for each individual improved. They thus began spawning at younger ages.

(5) Maturation of chub mackerel

Mean GSI of females sampled was 2.5. Histological examinations showed that the percentage of females which reached at yolk globule stage was 25% and that other females were at maturity stages former than that. No postovulatory follicle was observed in the ovaries. The plasma estradiol - 17 β (E_2) and 17 α , 20 β - dihydroxy 4 - pregnen - 3 - on (diOH) were at extremely low levels. Usually, chub mackerel start to spawn in April later than sardine. Also in this cruise in March, chub mackerel around Izu Islands were immature, while sardine spawned actively as shown above.

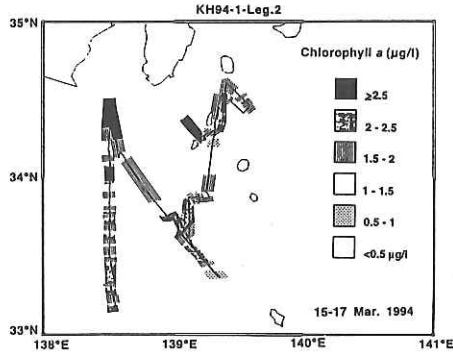


Fig. 1. Distribution of chlorophyll-a

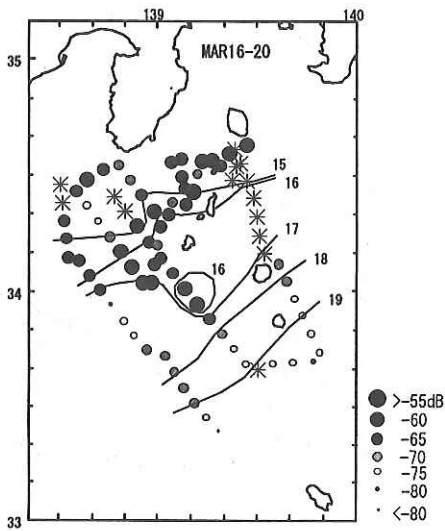


Fig. 2. Distribution of SV from zooplankton (10-50m depth, 5nm segment). SV values in daytime segments are shown and asterisks indicate nighttime segments excluded in analysis.

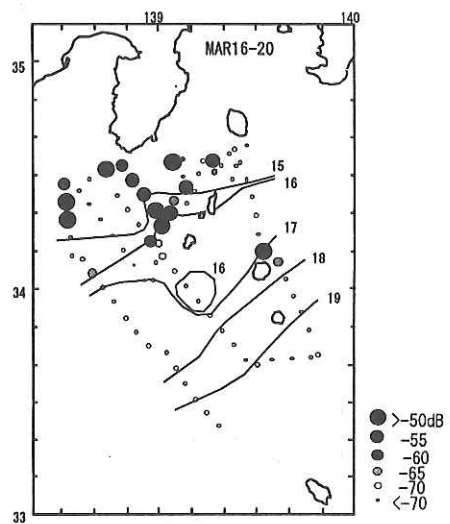


Fig. 4. Distribution of area backscattering strength (SA) from fish schools (10-50 m depth, 5nm segment).

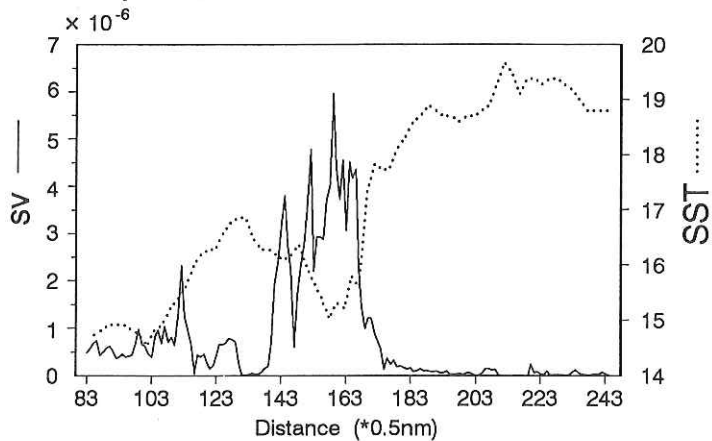


Fig. 3. Time series data of volume backscattering coefficient (sv) and sea surface temperature (SST) along middle the transect across the Kuroshio shown in Fig. 2.

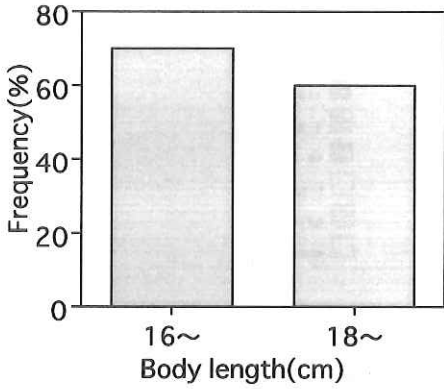


Fig.5. Percentages of individuals participating in spawning in the sea around of Izu islands, by body length.

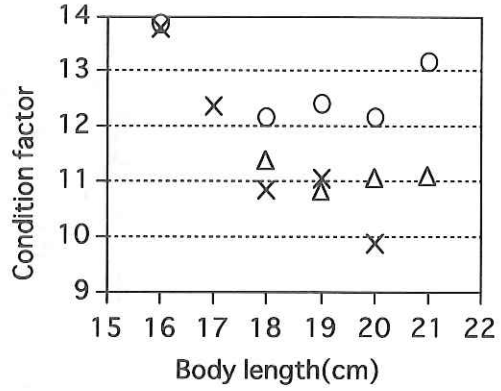


Fig.6 Condition factor for each body length.
 X: The sea around of Izu islands (March).
 O: The sea around of Izu islands (April).
 Δ: In the Tosa Bay (March).

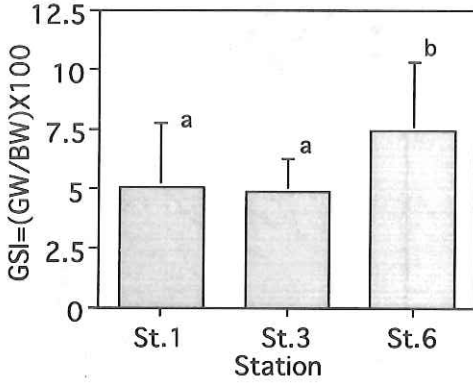


Fig.7 GSI differences for each station in Tosa Bay. Values show the mean \pm standard deviation. The mean values with the same superscript letter were not significantly different at the 5% level using Duncan's multiple range test.

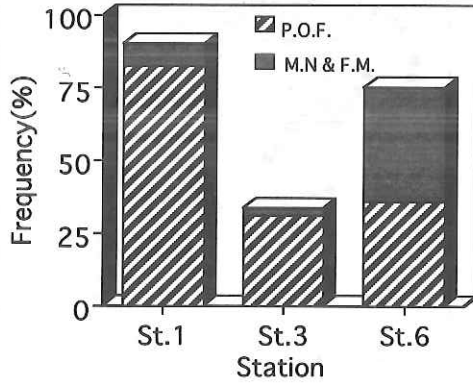


Fig.8 Percentages of individuals by each station participating in spawning in Tosa Bay. N.N.: Migratory nucleus stage. F.M.: Final maturational stage. P.O.F.: Post ovulatory follicle.

Distribution of plankton and micronecton by acoustic remote-sensing

Tadashi Inagaki and Kazushi Miyashita

Ocean Research Institute, University of Tokyo

Plankton and micronecton occupy an important position as bait of necton. A acoustic survey using 4 frequencies (38, 50, 120, 200 kHz: Acoustic Biomass Investigation System FURUNO) was carried out to investigate distribution of plankton and micronecton, quantitative evaluation and connection with distribution of necton in this cruise. Acoustic survey carried out in all line of this cruise, but in particular Kuroshio Current front of Tosa offing was paid attention to, and station was set at 1.5 n.miles spot of front both sides, and an acoustic measurement and the following work were carried out.

1. CTD (200 m) ; Correspondence with organisms distribution and physical environment structure , and acoustic data revision.
2. ORI net ; Correspondence with biomass and acoustic data.
3. MTD and IKMT; Examination of net avoidance by organisms size.

As a result of acoustic measurement in night time, a different aspect was shown to vertical distribution to 100 m of SV of 50 kHz in station of Kuroshio Current front both sides of Tosa offing. SV in Tosa side had stratified for the depth, and SV of surface layer region was most high. On the other hand, a value uniform comparatively was shown for depth direction in the Kuroshio Current side.

As a result of these, organisms concentrated on surface layer region in Tosa side, and that organisms was distributed over a way of roughly to 100 m in the Kuroshio Current side was suggested. And, average SV to 100 m of Kuroshio Current side was higher than that of Tosa side, and that total biomass was high was suggested.

Seawater sampling for elements-analysis using ICP-spectrometer

Manabu Shiraishi

National Research Institute of Aquaculture

The objectives of this thesis are to check by means of an Inductively Coupled Plasma Atomic Emission Spectrometry (ICP system) the distinctive characteristics of sea areas according to the quantity of each seawater trace element. On this voyage we conducted a preliminary study regarding the trace elements that can be used as indices to identify seawater's distinctive characteristics.

At each ocean station we collected seawater samples at 10 m intervals to depth of 100 m using Bandon seawater sampler. We filtered 500 ml of the water from each sample collected, using 0.45 and 0.22 μ m Millipore filters. The filtered seawater was stored in a cooled storage room at 5 °C. After disembarking we used the ICP system to measure the quantities of six elements: Magnesium (Mg), Calcium (Ca), Kalium (K), Strontium (Sr), Silica (Sil), and Sodium (Na).

No great difference was found in the quantities of Mg, Ca, K, and Sr for each station and water depth. For these elements there exist no distinctive sea-area characteristics. The values of Ca and Na varied at individual stations, showing differences that indicated a distinctive character for Sil to be slightly higher in depths of 50 m or more at station G-1 in Tosa Bay. Generally the content of Sil can easily be affected by the proximity of land, and there exists a tendency for the quantity of Sil to be higher in areas near land. Station G-1 is close to land, and the water depth in these areas is as shallow as 100 m. This is considered to be the reason why the amount of Sil in these areas was slightly higher than elsewhere. In the Kuroshio area, the measured value of Sil in the surface layer was small, and the measured Sil values rose as water depth increased (Increase in volume as water becomes deeper is a distinctive characteristic of Sil.). Sil quantities were small in areas where the water depth was shallow. The reason for this is assumed to be that Sil is consumed by diatoms.

We think that Sil can be used as an index if a detailed investigation of its distribution were conducted by increasing the number of ocean stations. Sil is known, however, to exist in two forms, that of biological origin and that of mineral origin. Accordingly, we must distinguish between the two. To understand the distinctive characters of sea areas, we must check many trace elements, including P.

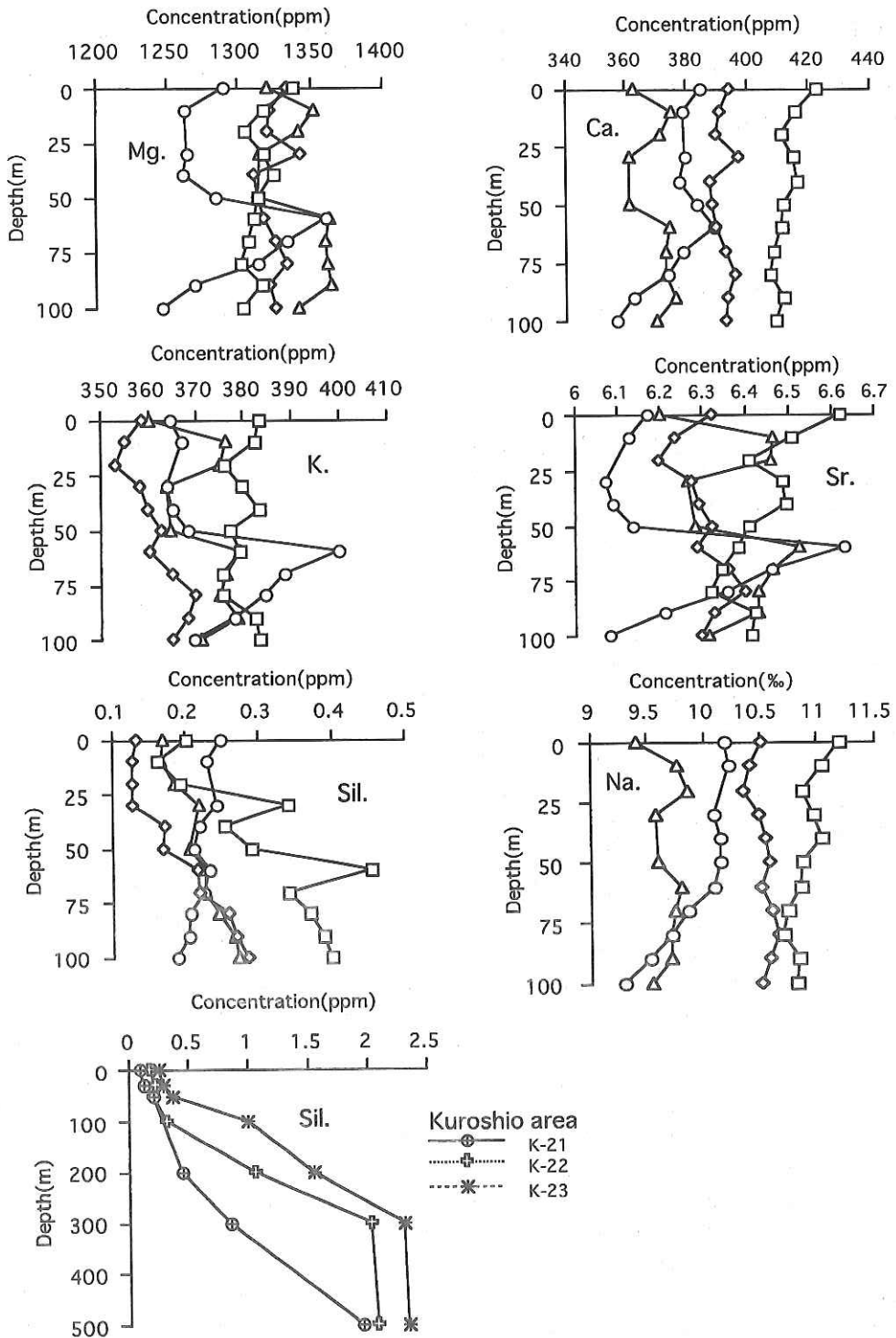


Fig.1 Differences in individual trace-element quantities each station.

—□— G-1 —◇— G-3 —○— G-9 —△— G-13

Spawning frequency and batch fecundity of the Japanese anchovy *Engraulis japonicus* caught at the nearshore of Miyake Island

Y. Tsuruta¹ and H. Niwa²

¹Hokkaido National Fisheries Research Institute

²Research Institute of Fisheries Engineering

Knowledge on the reproductive biology of the Japanese anchovy in the offshore area is important on considering the ecological role of them as the trigger at the beginning of the population increase, though being relatively scarce. In this report, we described some reproductive traits about the spawning frequency and batch fecundity.

Adult anchovy were sampled from 1930 to 2200 h by a gill net with 21mm and 26mm mesh aperture, which was set at 10-15 m depth, at the nearshore of Miyake Island, 34° 10' N, 139° 33' E, in March 18, 1994 (Fig.1). The fish were measured for body length, body weight and gonad weight. The gonads were fixed in 10% formalin, sectioned at 8 μ m and stained with hematoxylin/eosin for histological analysis. Maturity stage of each ovary was examined under a microscope for estimating the spawning frequency from the fraction of mature female spawning per day. A portion (about 0.1 to 0.3 g) of the hydrated ovaries were also preserved in 10% formalin for count of batch fecundity. Oocytes in the ovaries were completely separate, and the number of oocytes in the most advanced mode was counted under a microscope.

Body length composition: The body length of the anchovy ranged from 11.5 to 14.4cm with a mode of 13cm (Fig.1) which has scarcely appeared in the coastal area, recently. This mode of body length was larger than that (12cm mode) of anchovy sampled off Sanriku in 1991 (Tsuruta and Takahashi in press).

Spawning incidence: The maturity stages of ovaries and spawning features of the female anchovy are given in Table 1. The maturity stages were composed of the late yolk stage and the mature stage. The migratory nucleus stage did not occur. Moreover, the postovulatory follicles also did not appear. The postovulatory follicles occurred approximately between 2000 and 2200 h and degenerated within 24 h after spawning under experiment (Tsuruta and Hirose 1985). Therefore, it was suggested that spawning time was 1-2 h later than that (20-22 h) in Sagami Bay (Tsuruta and Hirose 1989). Since the postovulatory follicles were not observed in this survey, spawning frequency was estimated by dividing the number of the fish with the mature stage's ovary by the number of female specimen. The spawning frequency in the nearshore of Miyake Island was 0.27, which was low value as compared with that of fish sampled off Sanriku. Interspawning interval was estimated to be 3.7 days from the spawning incidence. It was longer than that off Sanriku, but it was almost the same as those of fish examined in April in Sagami Bay (Tsuruta and Hirose 1989). The gonosomatic indices of fish with mature stage's ovaries varied from 9.4 to 25.9 (Fig2),

which suggested that fish has already spawned several times in this spawning season.

Batch fecundity: Batch fecundity of fish caught at the nearshore of Miyake Island showed a slightly smaller number than that off Sanriku(Fig.3). However, there was no significant difference between two lines($p > 0.05$).

Table 1. Comparison of the composition of maturity stages and the spawning frequencies of the females Japanese anchovy caught at nearshore of Miyake Island and in the transition area off Tohoku Region.

Maturity stage	Location	Nearshore Miyake Island	Off Tohoku Region
		34° 10'N, 139° 33'E	37° 30'N, 166° 00'E
	Net setting time	19:30- 21:50	16:50- 18:15
	Water temp. (°C)	17.4	16.0
Early yolk stage		0(0)*3	3(5)
Late yolk stage		73(40)	25(40)
Migratory nucleus stage		0(0)	9(15)
Mature stage		27(15)	62(99)
Spawning frequency*1		0.27(55)	0.59(159)
Interspawning interval*2		3.7	1.7

*1 (Number of female with migratory nucleus and mature oocyte)/(total number of female in specimens).

*2 $1/(\text{spawning frequency})$.

*3 Number in parentheses indicates number of females in specimens.

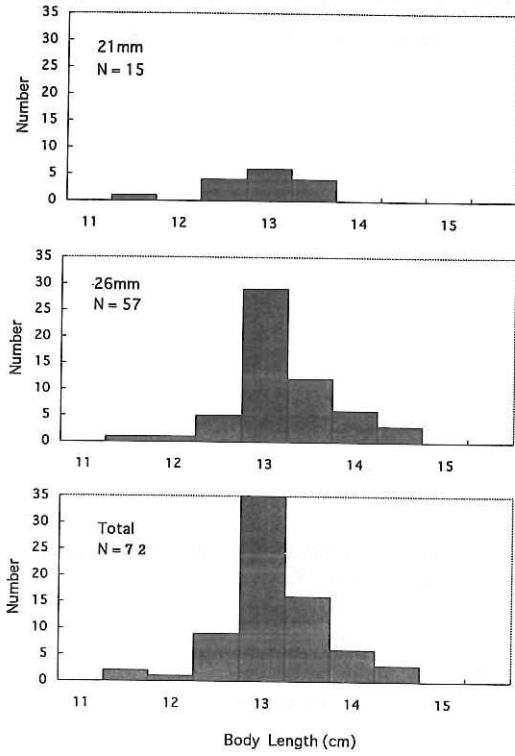


Fig.1. Distribution of body lengths of the Japanese anchovy caught by a gill net with two different meshes.

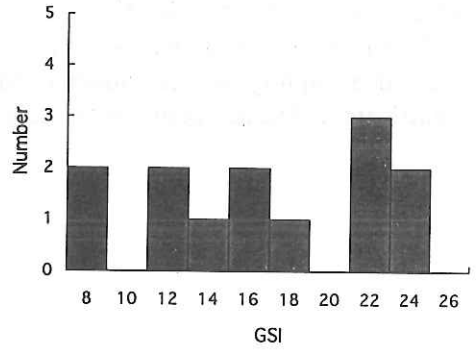


Fig.2. Distribution of gonosomatic indices of fish with hydrated ovary.

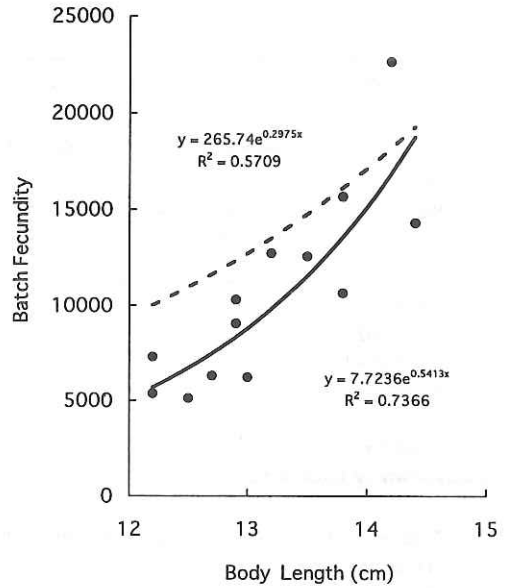


Fig.3. Comparison of batch fecundities between the groups collected at the nearshore of Miyake Island (solid line) and off Sanriku , 37° 30' N, 166° 00' E(dashed line).

Physical and biological fine structure in the Enshu-nada Sea

S.Kimura, H.Nakata and T.Sugimoto

Ocean Research Institute, University of Tokyo

Cyclonic circulations in frontal eddies associated with the wave-like meander of the western boundary current have been well described from satellite imagery and hydrographic observations, particularly in the Gulf Stream front between the Florida Strait and Cape Hatteras. In the region, meanders with several hundred kilometers wavelength and amplitudes of a few tens of kilometers propagate to the northwest. The southward movements of the tongue-like extrusions of the Gulf Stream derived from the wave crest generate a cold upwelled core in the wave trough with a few week period.

Similar frontal disturbances are also recognized in the Kuroshio region off the Japanese Pacific coast, as counterpart of those in the Gulf Stream in the Atlantic Ocean, and generate frontal cyclonic eddies frequently. These eddies supply nutrients to the euphotic layer by upwelling and accelerate primary production in the frontal region. The estimated annual carbon production by phytoplankton in the Kuroshio front is about $40 \text{ gC m}^{-2} \text{ y}^{-1}$, which is quite similar to the estimation in the Gulf Stream front.

In this cruise, we observed the vertical and horizontal fine structure of cyclonic eddies caused by frontal disturbances in the Kuroshio to describe their contribution to primary and secondary productions in the coastal area. In addition, we will look at the implication of the production enhancement due to the cyclonic eddies for the recruitment processes of Japanese anchovy, which has a major spawning ground in the Enshu-nada Sea.

Observations

Hydrographic observations with a conductivity-temperature-depth profiler (CTD, maximum depth was 500 m; the data can not be used for absolute values because of malfunction of CTD) and water sampling (0, 30, 50, 100, 200, 300, 500 m) were carried out in the Enshu-nada Sea along four sections twice (leg 1 and leg 2) in March, 1994 as shown in Figure 1.

Fine observations were made along 138E section where the eddies are frequently generated. In the section, surface net sampling with ORI33 net, multi-layer net sampling with MTD net and oblique towing with IKPT net (0.5mm mesh, wire out 200 m) were carried out during 5-6 and 14-15 March to collect macrozooplankton, fish eggs and larvae.

Results

During the both observations, the Kuroshio showed a small meandering off the Enshu-nada Sea with a 200 km wavelength. According to the surface temperature observed by satellite images, a large cold core with about 80 km diameter was recognized in leg 2 (Figure 1(b)). The location of this eddy coincident with upwelling feature as seen in the temperature

profile (Figure 2). The size was quite similar to that described by previous studies. On the other hands, small eddies with about 20 km diameter were observed in leg 1 (Figure 2(a)). For the first step, we focused the small eddies. The vertical profiles of temperature and chlorophyll-a concentration obtained in leg 1 are shown in Figure 3. Corresponding to the small cold cores, uplifted isotherms are recognized between Stations 30 and 31, and between 25 and 26. Although the eddies do not have large vertical structure, locations with high chlorophyll-a concentration greater than $2.0 \mu\text{g}/\ell$ were corresponding to those with the uplifted temperature pattern. It suggests that the water uplifted causes large upward nutrients transport and this may contribute to acceleration of phytoplankton growth. The high productivity extended to 50 m depth, although it was not recognized at 100 m depth. The biological productivity enhanced by the small cyclonic eddies did not spread over largely. However, the concentration is as same order as that in the large eddy with 80 km diameter previously observed. It means that the biological production by the small eddies can not be neglected in the estimation of total biological production in this region.

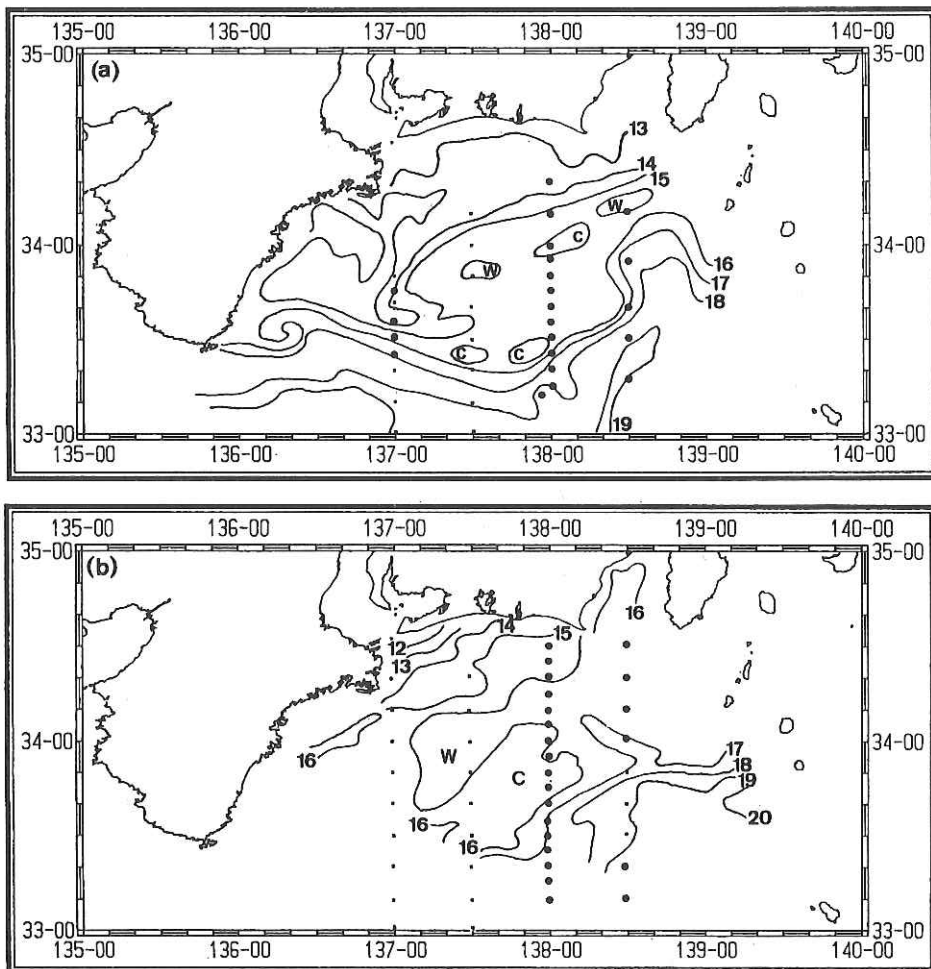


Figure 1 Observational locations with CTD (solid circles) and XBT (small dots) in leg1 (a) and leg2 (b). Contours indicate the sea surface temperature in °C observed by satellite.

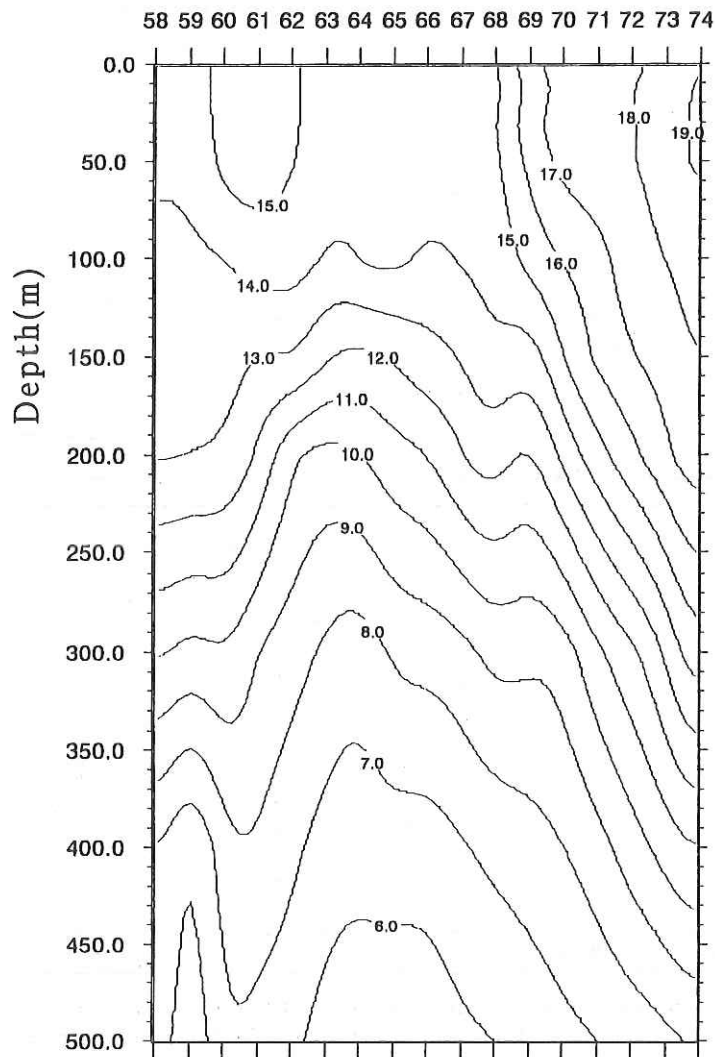


Figure 2 Vertical temperature (°C) section along 138°E in leg2. Station 58 is located in the most northern station.

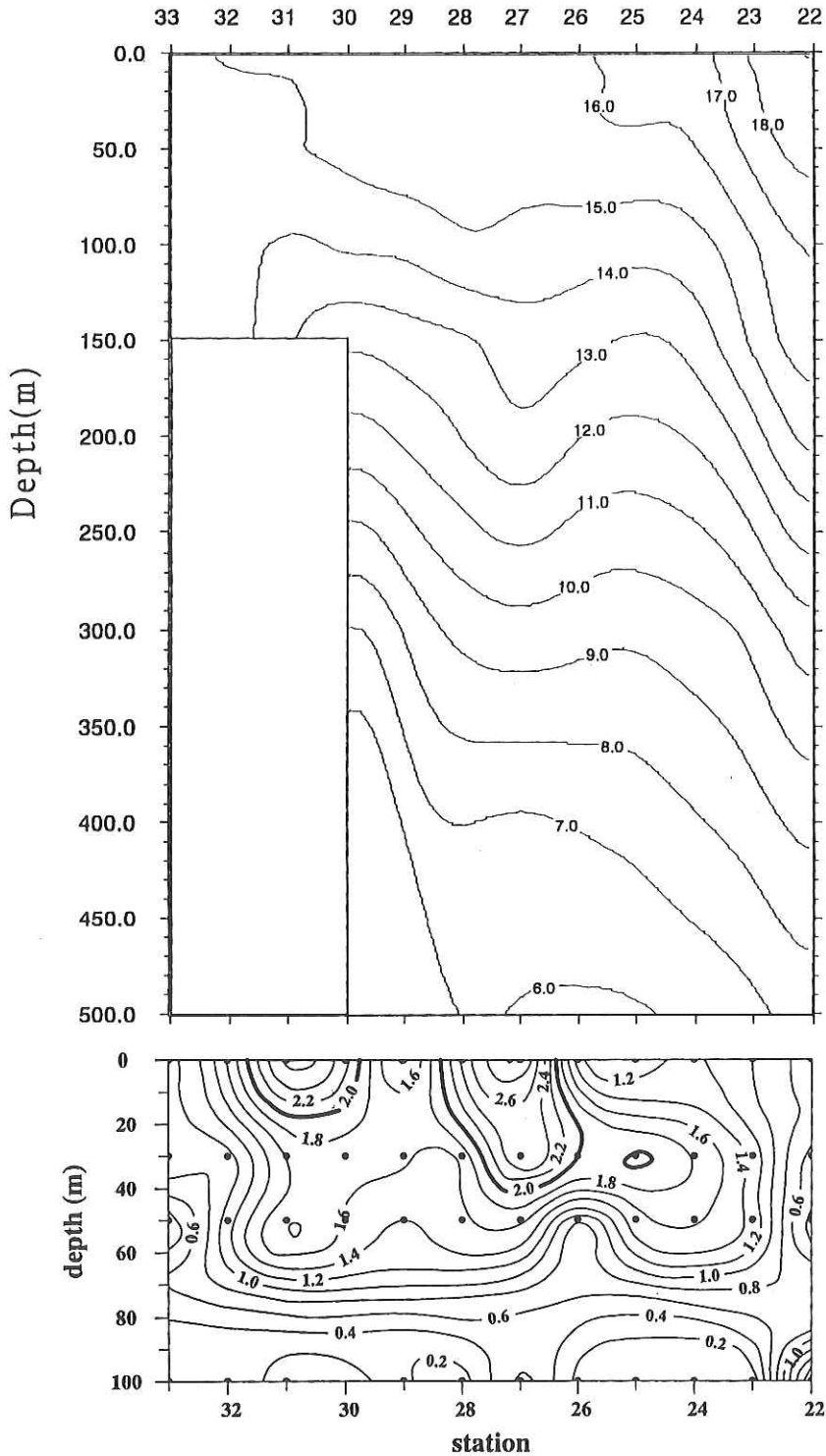


Figure 3 Vertical sections of temperature ($^{\circ}\text{C}$) and chlorophyll-a concentration ($\mu\text{g/l}$) along 138°E in leg1. Station 33 is located in the most northern station.

Estimation of volume, heat and salt transports across the Kuroshio off Cape Ashizuri

H. Ichikawa¹, N. Gohda², T. Tamura³ and T. Fujimoto³

¹Faculty of Fisheries, Kagoshima University.

²Faculty of Engineering, Hiroshima University.

³Graduate School of Engineering, Hiroshima University.

Introduction

The Kuroshio is the western boundary current of the North Pacific Subtropical Gyre and it is believed to play an important role in the poleward transports of heat and freshwater. However, their absolute values have not been determined accurately because it has been too difficult to measure absolute current velocity whole over the section across the Kuroshio. From 1991, the international WOCE (World Ocean Circulation Experiment) programme was started for understanding the role of ocean circulation in the global climate change by estimating the absolute values of oceanic transports of heat and salt.

As one of Japanese contribution to international WOCE programme and international GOOS (Global Ocean Observing System) programme, a large number of scientists from many universities and governmental agencies in Japan and University of Rhode Island in the U.S.A. participated in the Affiliated Surveys of the Kuroshio off Cape Ashizuri (ASUKA). One objective of this project is to establish a method to monitor the absolute values of volume, heat and salt transports of the Kuroshio by integrating the data obtained by moored instruments, the CTD/XBT and towed-ADCP data obtained frequently as much as possible by ships and the sea surface altimetry data by TOPEX/POSEIDON satellite. The other is to estimate the meridional heat and salt transports of the North Pacific Subtropical Gyre combining the data at ASUKA-line with the hydrographic data at the 30° N Trans-Pacific line obtained by Japanese oceanographers from December 1993 to February 1994.

In October 1993, 33 Aanderaa current-meters, 2 upward-looking ADCPs and 8 IESs were deployed by T/V *Keitenmaru* of Kagoshima University along the ASUKA-line. During 2-year long intensive survey period from October 1993 to November 1995, the ASUKA Group carried out CTD/XBT observations 40 times and towed-ADCP measurements from ships 12 times including our KH94-01 cruise.

In this report, we describe preliminarily the current velocity data obtained by towed-ADCP measurements and two temperature sections by XBT/CTD observations only in the KH94-01 cruise together with a note on the experimental error in the temperature section caused by internal tide.

Velocity section measured by towed-ADCP

Towing the ADCP (RDI-0150DR) with communication cable and rope of 70 m long, we

obtained current velocity data with depth interval of 8 m in the top 280 m layer from Stn.AS02 at 23:35 (JST) on February 26 to AS14 at 21:25 on February 27 without any trouble. During the measurements, the ship speed had been kept 8 knot and north and east components of horizontal current velocity, vertical velocity, intensity of back scattering and water temperature at the depth of ADCP of about 6 m were recorded every minute together with ship's position by GPS every three seconds.

Figure 1 shows distributions of spatial-averaged current vectors at every 16 m in depth and water temperature at about 6 m depth along ASUKA-line. This figure indicates that the current vector was nearly uniform in vertical direction over the whole section while vertical bearing of current vector existed in the upper 100 m layer near Stns.AS09, AS11 and AS13. Figures 2 and 3 show the vertical sections of ENE-component (perpendicular to the ASUKA-line, i.e., nearly parallel to the Kuroshio) and SSE-component (parallel to the ASUKA-line) of current velocity, respectively. In Fig.2, we can find that the Kuroshio axis was located between Stns.AS04 and AS05 and its maximum velocity reached up to larger than 100 cm sec^{-1} in the top 200 m layer. The counter current existed between Stns.AS09 and AS13 and had its maximum value larger than 20 cm sec^{-1} near Stn.AS12. The current velocity component parallel to the ASUKA-line had negative value in the whole section in Fig.3. This suggests that a center of anticyclonic eddy was located in the east of the ASUKA-line.

From Fig.2, the ASUKA-line from Stn.AS02 to Stn.AS14 can be divided into three regions, i.e., the main stream region of the Kuroshio from Stn.AS02 to Stn.AS06, the transition zone from Stn.AS07 to Stn.AS09 and the Kuroshio Counter Current region from Stn.AS09 to Stn.AS14. The volume transport in the top 250 m layer is estimated to be 17.2 Sv ($1 \text{ Sv} = 10^6 \text{ m}^3 \text{ s}^{-1}$) in the main stream region of the Kuroshio, 4.1 Sv in the transition zone and -5.1 Sv in the Kuroshio Counter Current region.

Temperature Sections measured by XBT/CTD

During outgoing trip from Stn.AS01 at 21:14 on February 26 (JST) to Stn.AS14 at 21:00 on February 27, 18 XBT probes were launched with keeping ship speed to be 8 knot. During return trip from AS13 to AS01 at 21:07 on February 28, CTD lowerings were made at 9 stations and 5 XBT probes were launched. Due to malfunction of CTD system, only vertically-averaged temperature over 9 m depth were obtained every 1 m at CTD stations. Figure 4 shows the vertical section of temperature in the top 750 m layer measured by XBT during outgoing trip, and that measured by CTD or XBT during return trip. Both of the two sections indicate the typical features of temperature section across the Kuroshio. Comparing two sections, the front at Stn.AS04 in outgoing trip has moved onshoreward by about 40 km to Stn.AS02 in return trip, suggesting that the Kuroshio axis had moved toward NNW with a speed of about 20 km day^{-1} .

In outgoing trip, temperature is higher than 20°C in the top 200 m layer between Stns.AS05 and AS06 and a thermal front is dominant in its onshore area. Surface mixed layer temperature is lower than 19°C between Stns.AS09 and AS12. This temperature distribution in the upper layer is corresponding well with the velocity section shown in Fig.2, e.g., the current speed is maximum in the thermal frontal region, the highest temperature water exists in the offshore-side of the Kuroshio axis, and the surface mixed

layer temperature is lower than 19°C in the counter current region.

Isotherms lower than 14°C are deepest at Stn.AS09 in outgoing trip but at Stn.AS10 in return trip. Amplitude of undulation of isotherms seems to have increased in return trip especially at Stn.AS13. Vertical displacement of isotherm is dominated by internal tide. Therefore, these results should be apparent features caused by experimental error due to differences of time interval of observations conducted during each trip and time of each observation. In order to calculate the geostrophic volume transport accurately from hydrographic data, we have examined contribution of time-dependent component to the observed spatial variation with assuming that observed temperature T_{obs} at different station in different time can be represented by (1).

$$T_{obs}(x, z, t) = T_x(z, x) + T_t(z, t), \quad (1)$$

where

$$T_x(z, x) = a_1(z)x^3 + a_2(z)x^2 + a_3(z)x + a_4(z), \quad (2)$$

$$\begin{aligned} T_t(z, t) &= T_{obs}(x, z, t) - T_x(x, z) \\ &= A_1(z)\sin(n_1 \omega t) + A_2(z)\cos(n_1 \omega t) + A_3(z)\sin(n_2 \omega t) \\ &\quad + A_4(z)\cos(n_2 \omega t) + A_5(z)t + A_6(z) \end{aligned} \quad (3)$$

Here, x, t , and z are the distance from Stn.AS01 along the ASUKA-line, the observation time from 09:00 on February 26 and the depth, respectively. T_x and T_t are respectively the time-independent and time-dependent components of T_{obs} , ω the angular frequency of diurnal tidal period, and n defines tidal period considered. We calculated the coefficients $a_1 \dots a_4$ in (2), and then the coefficients $A_1 \dots A_6$ in (3) by the least square method at each depth. Estimated best fit values of T_x and $T_x + T_t$ at 450 m depth of Stns.AS09 - AS14 are shown in Fig.5 together with T_{obs} . It is obvious that large differences between temperatures during outgoing and return trips and small-scale spatial variation of temperature can be attributed to internal tide.

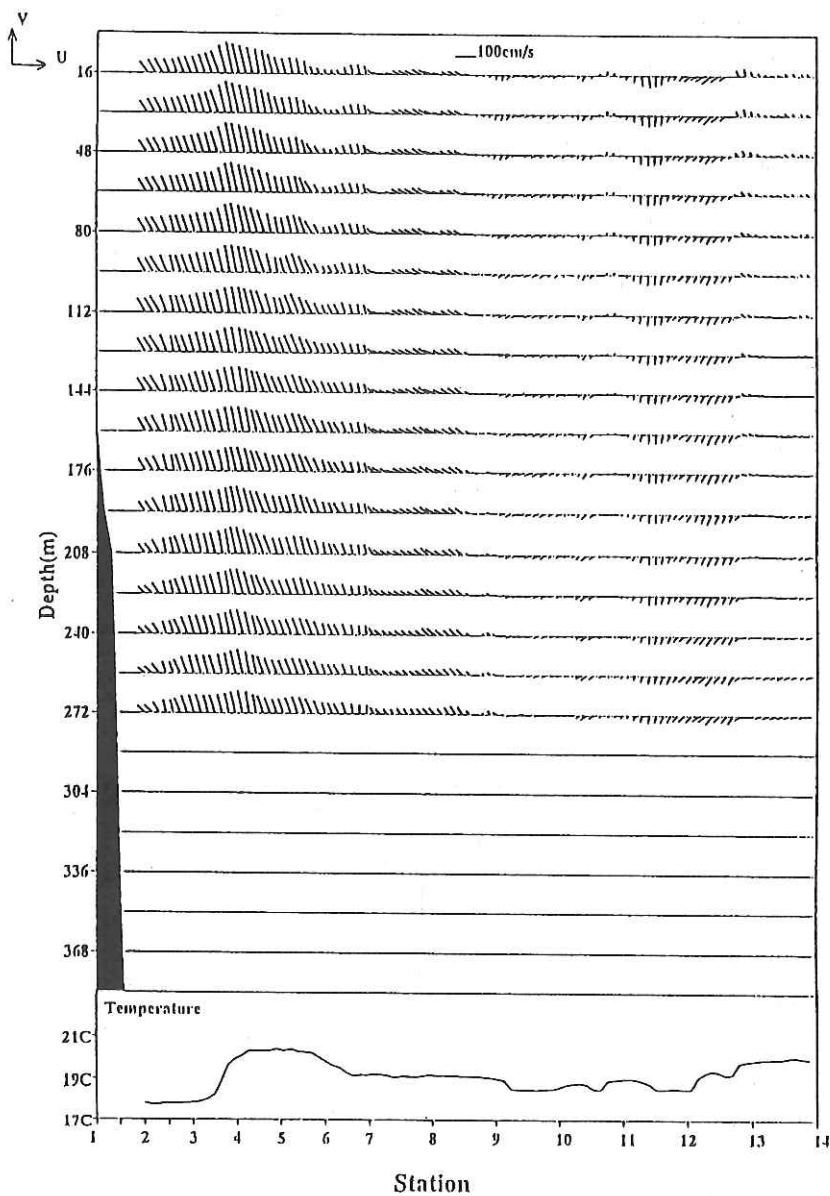


Figure 1. Stick diagram of spatial-mean current vectors at every 16 m in depth and water temperature at about 6 m depth measured by towed-ADCP along ASUKA-line. U and V are the velocity components parallel (toward ENE) and perpendicular (toward SSE) to the ASUKA-line, respectively.

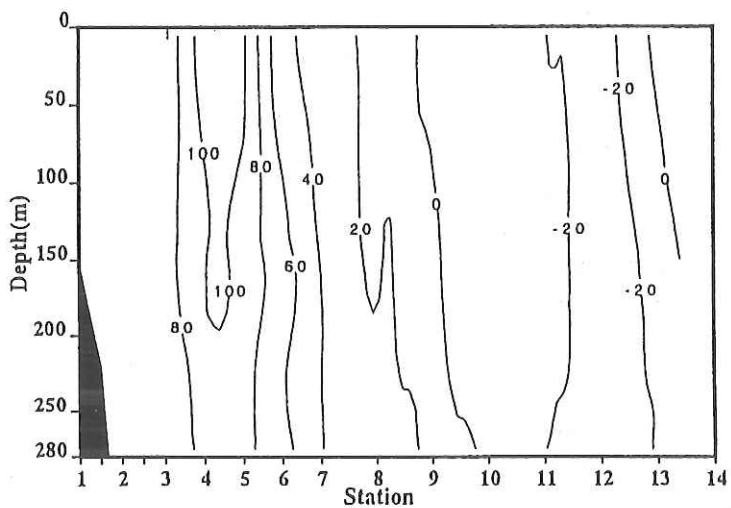


Figure 2. Isopleths of velocity component perpendicular to the ASUKA-line in cm sec^{-1} . Positive value indicates current toward ENE, the current direction of the Kuroshio.

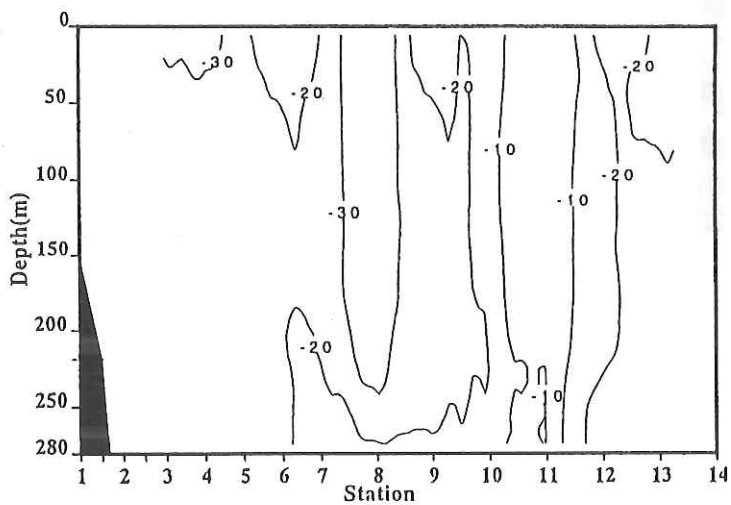


Figure 3. Isopleths of velocity component parallel to the ASUKA-line in cm sec^{-1} . Positive value indicates current toward SSE, the offshoreward direction from the Cape Ashizuri.

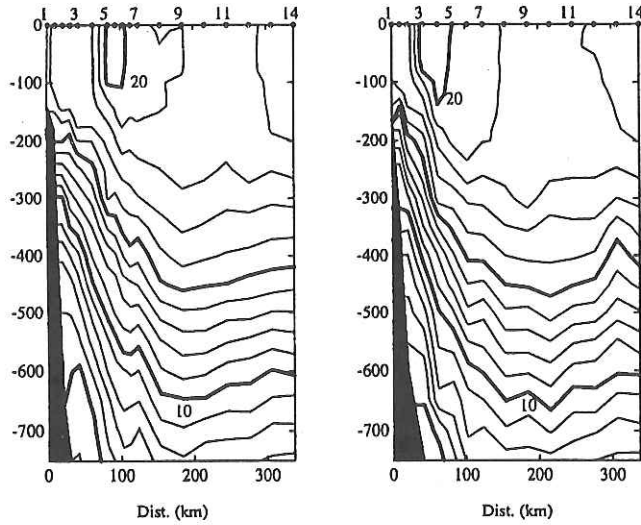


Figure 4. Vertical sections of temperature in °C over the ASUKA-line. Left panel: outgoing trip from Stn.AS01 at 21:14 on February 26 (JST) to Stn.AS14 at 21:00 on February 27, Right panel: return trip from Stn.AS14 at 21:00 on February 27 to Stn.AS01 at 21:07 on February 28.

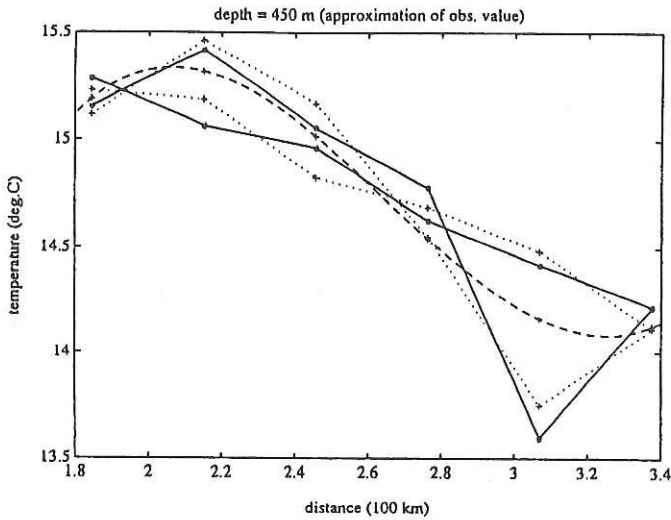


Figure 5. Best fit values of estimated temperatures for $n_1 = 2$ and $n_2 = 3$ in (3) at 450 m of Stns.AS09 – AS14 with observed values. Full line: T_{obs} , Broken line: T_x , Dotted line: $T_x + T_t$ (See text for explanation).

Aerosol particle concentration over the south ocean of Japan Islands in winter

K. Miura¹, H. Kojima², K. Matsuda¹, M. Hidaka¹, and S. Nakae¹

¹ Department of Physics, Faculty of Science, Science University of Tokyo,

² Department of Liberal Arts, Faculty of Science and Technology, Science University of Tokyo

Introduction

Atmospheric aerosol particles give rise to both direct and indirect effects on the climate. The direct effects of atmospheric aerosols on the climate are that aerosols absorb and scatter both solar and infrared radiation. The indirect effects are the influence on the process of cloud formation.

We have measured background aerosol particle concentration on board by the R/V Hakuho Maru in our five expeditions (KH-89-T3, KH-89-2, KH-91-5, KH-92-5, KH-93-3). We reported the global map of Aitken particles drawn by our three expeditions' data in addition to other workers' data (Miura *et al.*, 1993). However, these expeditions were carried out in summer or autumn. In this expedition, we first measured particle concentration in winter over the south ocean of Japan Islands. We also collected aerosols on filters and on a carbon-covered nitrocellulose film supported on an electron microscopic grid.

Moreover, we observed solar radiation and measured several gases. In this report, we describe the concentrations of aerosol particles and radon over the ocean transported from Japan Islands.

Methods

Counting of aerosol particles was carried out with two counters on an upper deck, being about 15 m above the sea surface and in the direction of 30 degrees left from the front of a funnel. Aitken particle concentrations ($r < 0.1 \mu\text{m}$) were measured with a Pollak condensation nuclei counter. Larger particle concentrations ($r > 0.15, 0.305, 0.615, 1.25, 2.5 \mu\text{m}$) were measured with an optical particle counter (KC01, Rion Co. Ltd.). We used concentrations larger than 0.15 and 1.25 μm in radius as those of large and giant particles, respectively.

High concentration of aerosol particles was sometimes caused by the exhaust of ship. To avoid exhaust gases of ship, we omitted the data measured during a calm (relative wind speed is less than 1 m/s) period or a period of blowing from the funnel.

Radon concentration was measured continuously by use of a radon monitor. The device was composed of an semi-spherical stainless steel chamber with a volume, 24 liters and a ZnS(Ag) scintillation detector for alpha counting. A high voltage (2 kV) was applied between the chamber and the detector. The freshly formed RaA atoms which are

positively charged were deposited on the detector covered with a thin aluminum foil and the alpha activity from the nuclide was counted. The radon concentrations were calculated based on a Bateman equation and the counts of the alpha for a hour.

Concentrations of individual radon daughter were also measured by a continuous radon daughter monitor. In the monitor, radon daughters were sampled on a membrane filter (1 μ m in pore size) on a roll type (60 mm in width and 10 m in length) and the gross alpha activity was counted a three different times. The first counting was done for 15 min while the air sampling was going on; the second and third countings were done for 20 min each in succession while the sampling was stopped. The individual concentrations of RaA, B and C were calculated from a Bateman equation and the three counting values.

Results and discussion

Radon gas, SO₂ gas, Aitken particle, large particle, and giant particle concentrations measured in the legs 1 and 2 were shown in Figs 1 and 2, respectively. These concentrations decreased as leaving from Tokyo. They were generally high near the Islands and low far from the Islands.

Figure 1 shows that the concentration of Aitken particles recorded the minimum value around 31 N in latitude. This station was the farthest station from the Islands in this expedition. This value was 100 to 400 particles/cm³, which was nearly equal to that measured over remote oceans (Miura *et al.*, 1993) and two and a half orders of magnitude lower than that measured in Tokyo (Miura and Sekikawa, 1990). Radon gas also showed the minimum value at the station. Radon is a tracer of continental air mass because it exhales from soil. This shows that Aitken particles over this ocean is mainly transported from the Japan Islands.

However, large and giant particles didn't show the minimum value at that station. These particles were not only transported from the Islands but also generated from sea surface as seasalt particles. Particle concentration in the marine boundary layer, N is given as

$$\frac{dN}{dt} = Q - \lambda_{dec}N - \lambda_{dil}N + \lambda_{dil}N_b, \quad (1)$$

where N_b is particle concentration in the free atmosphere, Q is production rate, λ_{dec} is the decay rate, and λ_{dil} is the dilution rate. For large and giant particles $N_b \ll N$, so we can neglect the forth term. Putting $\Lambda = \lambda_{dec} + \lambda_{dil}$,

$$\frac{dN}{dt} = Q - \Lambda N \quad (2)$$

Solving Eq. (2) at the condition $N = N_0$ ($t = 0$),

$$N = \frac{Q}{\Lambda} \{1 - \exp(-\Lambda t)\} + N_0 \exp(-\Lambda t) \quad (3)$$

When $t \rightarrow \infty$, $N \rightarrow \frac{Q}{\Lambda}$ Eq. (3) shows that N decreases when $N_0 > \frac{Q}{\Lambda}$, but N increases

when $N_0 < \frac{Q}{\Lambda}$ Size distributions of $\frac{Q}{\Lambda}$ measured in this expedition were dependent wind force. They increased as wind force became strong. This relation has been

previously reported (*e.g.*, Kojima and Sekikawa, 1974; Miura *et al.*, 1995) . It suggests that the large and giant particles over this ocean are mainly seasalt particles.

More detailed analysis will be done by comparing with the other elements.

References

- Kojima, H. and T. Sekikawa, Some characteristics of background aerosols over the Pacific Ocean, *J. Meteor. Soc. Jpn.*, **52**, 499-505, 1974.
- Miura, K., Y. Hashizume, T. Sampei, and S. Nakae, Aerosol particle concentration over the western equatorial Pacific Ocean, *J. Atmos. Electr.*, **15**, 37-44, 1995.
- Miura, K., S. Nakae, T. Sekikawa, and T. Kumakura, Global distribution of Aitken particles over the oceans, *J. Atmos. Electr.*, **13**, 133-144, 1993.
- Miura, K. and T. Sekikawa: Variation of Concentration of Aerosol Particles at the Center of Tokyo, *Atmospheric Environment*, **24**, 1401-1408, 1990.

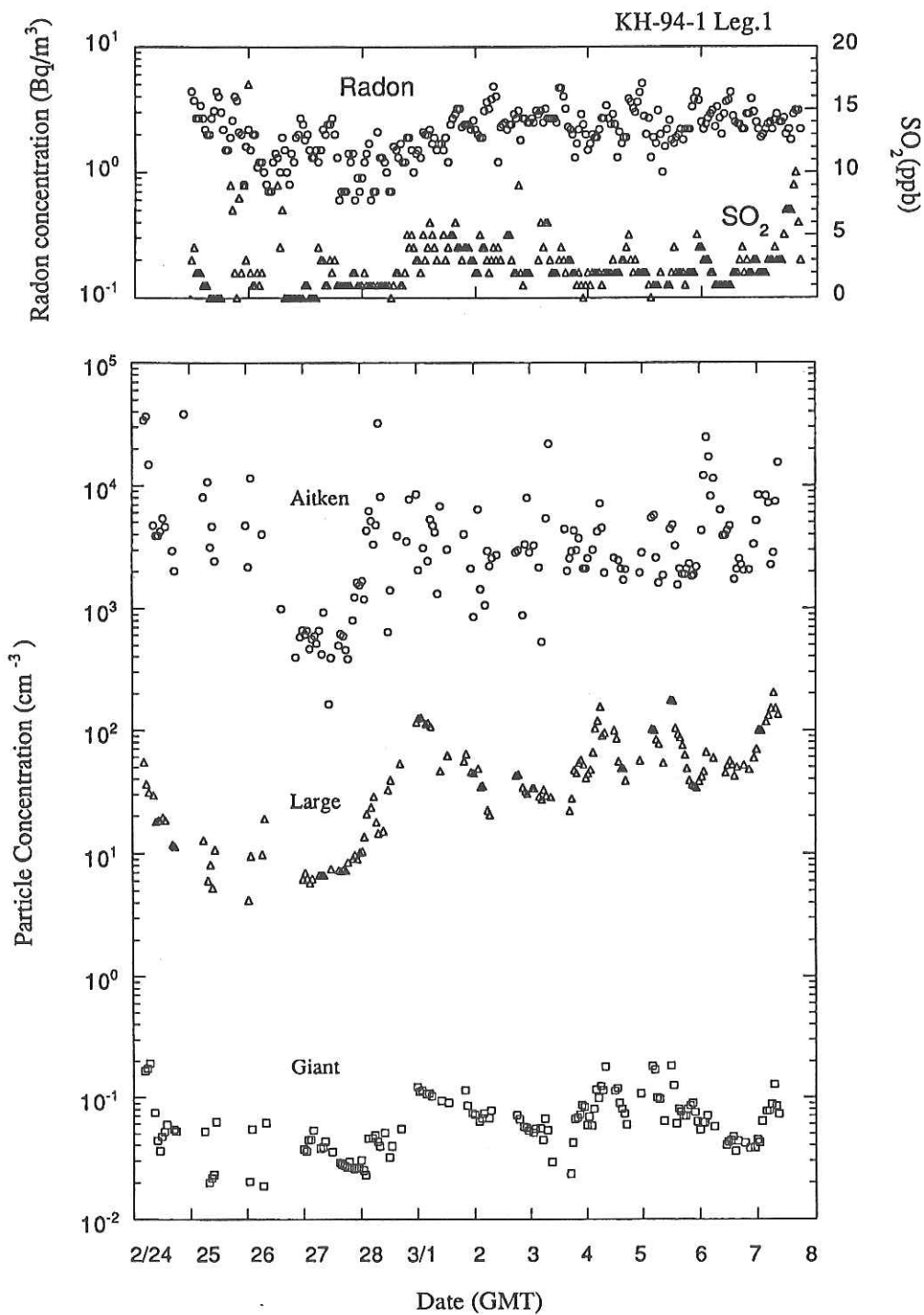


Fig. 1 The variations of concentrations of Radon gas, SO₂ gas, Aitken particles, large particles, and giant particles measured in the leg 1.

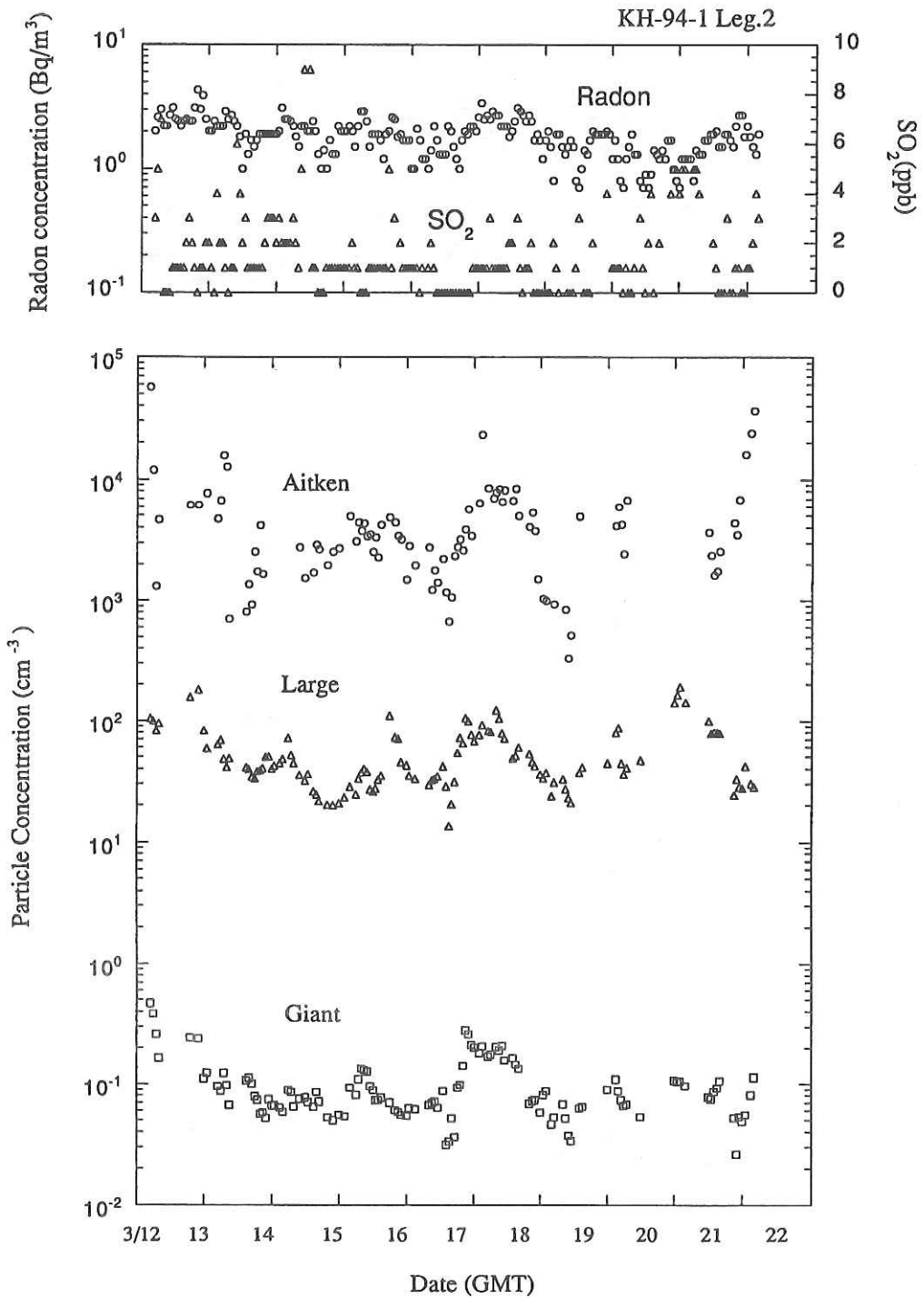


Fig. 2 The same as Fig. 1, but for the leg 2.

Y.M.D	JST	LAT.	LONG.	DEPTH	ST.NO.	COMENT
-------	-----	------	-------	-------	--------	--------

Leg 1:Set Sail from Tokyo to Yokohama

94.02.24	1400	35 38.540N	139 46.450E	0		
	1600	35 18.220N	139 43.960E	155		
	2000	34 32.000N	139 01.120E	137		
94.02.25	0000	34 08.600N	137 54.890E	811		
	0200	33 59.230N	137 29.870E	1610	K-1	
	0224	33 58.950N	137 29.590E	252	K-1	CTD START
	0253	33 58.330N	137 29.380E	527	K-1	CTD DEEPEST
	0308	33 58.130N	137 29.040E	1681	K-1	CTD FINISH
	0430	33 49.620N	137 30.150E	1828	K-2	CTD START
	0502	33 49.120N	137 29.930E	1845	K-2	CTD FINISH
	0620	33 39.980N	137 30.180E	3346	K-3	CTD START
	0637	33 39.700N	137 30.350E	3238	K-3	CTD DEEPEST
	0650	33 39.570N	137 30.610E	3254	K-3	CTD FINISH
	0817	33 29.880N	137 30.380E	3960	K-4	CTD START
	0835	33 29.730N	137 30.990E	3952	K-4	CTD DEEPEST
	0845	33 29.950N	137 31.530E	3933	K-4	CTD FINISH
	1015	33 19.880N	137 30.280E	3879	K-5	CTD START
	1030	33 20.000N	137 30.910E	3807	K-5	CTD DEEPEST
	1040	33 20.000N	137 31.380E	3796	K-5	CTD FINISH
	1200	33 10.710N	137 29.820E	3950		
	1207	33 10.410N	137 30.130E	3933	K-6	CTD START
	1224	33 10.510N	137 30.760E	3920	K-6	CTD DEEPEST
	1234	33 10.570N	137 31.160E	3917	K-6	CTD FINISH
	1400	33 00.150N	137 30.320E	3912	K-7	CTD START
	1415	33 00.060N	137 30.840E	3883	K-7	CTD DEEPEST
	1425	33 00.020N	137 31.210E	3887	K-7	CTD FINISH
	1600	32 59.970N	137 12.070E	4224		
	1644	33 00.230N	137 00.040E	4290	K-8	XBT
	1723	33 09.980N	136 59.940E	4058	K-9	XBT
	1801	33 20.040N	136 59.980E	2706	K-10	XBT
	1918	33 40.070N	136 59.850E	2018	K-12	XBT
	1956	33 49.950N	136 59.960E	2039	K-13	XBT
	2000	33 50.660N	137 00.310E	2007		
	2030	33 44.950N	137 00.020E	2016	K-14	CTD START
	2043	33 44.740N	136 59.980E	2016	K-14	CTD DEEPEST
	2050	33 44.700N	136 59.910E	2017	K-14	CTD FINISH
2056	33 44.640N	136 59.930E	2017	K-14	ORI SIDE NET START	
2113	33 44.010N	136 59.900E	2015	K-14	ORI SIDE NET FINISH	
2148	33 39.960N	136 59.990E	2020	K-15	CTD START	
2200	33 40.000N	136 59.740E	2019	K-15	CTD DEEPEST	
2207	33 40.040N	136 59.610E	2018	K-15	CTD FINISH	
2210	33 39.980N	136 59.520E	2019	K-15	ORI NET START	
2227	33 39.440N	136 59.290E	2023	K-15	ORI NET FINISH	

Y.M.D	JST	LAT.	LONG.	DEPTH	ST.NO.	COMENT
	2308	33 35.080N	137 00.050E	2047	K-16	CTD START
	2319	33 35.120N	136 59.970E	2047	K-16	CTD DEEPEST
	2326	33 35.160N	136 59.920E	2048	K-16	CTD FINISH
	2330	33 35.130N	136 59.890E	2047	K-16	ORI SIDE NET START
	2344	33 34.570N	136 59.840E	2049	K-16	ORI SIDE NET FINISH
94.02.26	0000	33 32.780N	136 59.960E	2046		
	0022	33 30.060N	137 00.040E	2057	K-17	CTD START
	0040	33 29.970N	137 00.170E	2059	K-17	CTD FINISH
	0045	33 29.920N	137 00.200E	2058	K-17	ORI SIDE NET START
	0057	33 29.320N	137 00.320E	2046	K-17	ORI SIDE NET FINISH
	0134	33 25.040N	137 00.060E	1969	K-18	CTD START
	0144	33 25.080N	137 00.330E	2150	K-18	CTD DEEPEST
	0150	33 25.060N	137 00.490E	2046	K-18	CTD FINISH
	0156	33 24.950N	137 00.650E	1926	K-18	ORI SIDE NET START
	0207	33 24.460N	137 00.860E	2000	K-18	ORI SIDE NET FINISH
	0247	33 20.260N	137 00.440E	2671	K-19	CTD START
	0259	33 20.110N	137 01.220E	2786	K-19	CTD DEEPEST
	0305	33 20.090N	137 01.640E	2824	K-19	CTD FINISH
	0310	33 20.040N	137 01.880E	2811	K-19	ORI SIDE NET START
	0321	33 19.520N	137 02.660E	3037	K-19	ORI SIDE NET FINISH
	0400	33 15.160N	137 01.720E	3432		
	0454	33 09.970N	136 59.910E	2901	K-20	CTD START
	0509	33 09.880N	137 00.700E	3124	K-20	CTD DEEPEST
	0516	33 09.920N	137 01.040E	3096	K-20	CTD FINISH
	0522	33 09.890N	137 01.380E	3068	K-20	ORI SIDE NET START
	0533	33 09.570N	137 02.000E	3424	K-20	ORI SIDE NET FINISH
	0800	33 05.960N	136 28.800E	2880		
	1200	32 59.750N	135 28.790E	2390		
	1600	32 53.340N	134 26.460E	1403		
	2100	32 45.230N	133 06.630E	174		
	2114	32 45.140N	133 05.970E	152	A0101	XBT
	2123	32 44.900N	133 06.160E	232		SET SPEED 8KT
	2202	32 39.980N	133 09.070E	220	A01A1	XBT
	2248	32 34.990N	133 12.090E	613	A0201	XBT
	2331	32 32.130N	133 13.680E	741		TOW ADCP
	2338	32 31.390N	133 14.150E	735		SET SPEED 8KT & s/co on 153°
	2350	32 29.990N	133 15.050E	805	A02A1	XBT
94.02.27	0000	32 28.900N	133 15.580E	890		
	0035	32 24.960N	133 18.060E	947	A0301	XBT
	0202	32 14.990N	133 23.120E	1166	A0401	XBT
	0337	32 04.980N	133 29.020E	1971	A0501	XBT
	0400	32 02.420N	133 30.570E	2131		
	0421	32 00.000N	133 31.980E	2269	A05A1	XBT
	0503	31 55.030N	133 34.000E	2975	A0601	XBT
	0546	31 49.980N	133 36.980E	3628	A06A1	XBT
	0627	31 45.000N	133 40.010E	4526	A0701	XBT

Y.M.D	JST	LAT.	LONG.	DEPTH	ST.NO.	COMENT
	0800	31 34.180N	133 45.790E	4878		
	0836	31 29.990N	133 48.020E	4844	A0801	XBT
	1045	31 14.990N	133 56.010E	4543	A0901	XBT
	1200	31 05.820N	134 00.940E	4466		
	1249	31 00.000N	134 04.050E	4440	A1001	XBT
	1449	30 44.990N	134 12.050E	4461	A1101	XBT
	1600	30 36.150N	134 16.840E	4494		
	1648	30 30.000N	134 20.040E	4534	A1201	XBT
	1655	30 29.220N	134 20.470E	4543	A1201	XBT AGAIN
	1657	30 28.920N	134 20.620E	4549	A1201	XBT
	1702	30 28.340N	134 20.940E	4555	A1201	XBT
	1856	30 15.000N	134 28.080E	4534	A1301	XBT
	2000	30 07.320N	134 32.150E	4626		
	2100	30 00.000N	134 36.070E	4637	A1401	XBT
	2110	29 58.760N	134 36.680E	4648		FINISH ADCP
	2215	30 00.340N	134 36.000E	4646	A1402	CTD-RMS START
	2243	30 00.630N	134 36.120E	4645	A1402	CTD-RMS DEEPEST
	2253	30 00.700N	134 36.130E	4645	A1402	CTD-RMS FINISH
94.02.28	0000	30 14.030N	134 28.490E	4510		
	0017	30 14.860N	134 28.000E	4519	A1302	CTD-RMS START
	0039	30 14.830N	134 28.010E	4525	A1302	CTD-RMS DEEPEST
	0119	30 14.940N	134 28.020E	4530	A1302	CTD-RMS FINISH
	0236	30 30.060N	134 19.920E	4532	A1202	XBT
	0338	30 45.040N	134 11.940E	4461	A1102	XBT
	0400	30 50.230N	134 09.230E	4451		
	0452	30 59.900N	134 04.040E	4431	A1002	CTD START
	0518	30 59.940N	134 03.700E	4435	A1002	CTD DEEPEST
	0532	31 00.000N	134 03.580E	4436	A1002	CTD FINISH
	0645	31 14.720N	133 56.040E	4540	A0902	XBT
	0755	31 30.120N	133 47.910E	4857	A0802	CTD-RMS START
	0821	31 30.240N	133 48.310E	4844	A0802	CTD-RMS DEEPEST
	0846	31 30.400N	133 48.660E	4848	A0802	CTD-RMS FINISH
	0958	31 45.020N	133 39.920E	4524	A0702	XBT
	1045	31 54.930N	133 34.230E	2957	A0602	CTD-RMS START
	1107	31 55.190N	133 34.720E	2953	A0602	CTD-RMS DEEPEST
	1126	31 55.330N	133 35.170E	2868	A0602	CTD FINISH
	1133	31 55.320N	133 35.290E	2874	A0602	RELEASE OF DRIFTING BUOY
	1142	31 55.350N	133 35.220E	2885	A0602	ORI SIDE NET START
	1152	31 55.500N	133 35.140E	2983	A0602	ORI SIDE NET FINISH
	1200	31 55.540N	133 35.230E	2989		s/co on 331°
	1257	32 04.810N	133 29.230E	1928	A0502	CTD START
	1319	32 04.750N	133 29.850E	1852	A0502	CTD DEEPEST
	1338	32 04.840N	133 30.260E	1883	A0502	CTD FINISH
	1447	32 14.870N	133 23.280E	1224	A0402	CTD-RMS START
	1508	32 15.070N	133 23.950E	1161	A0402	CTD-RMS DEEPEST
	1541	32 15.330N	133 24.710E	1156	A0402	CTD-RMS FINISH

Y.M.D	JST	LAT.	LONG.	DEPTH	ST.NO.	COMENT
	1545	32 15.340N	133 24.860E	1112	A0402	RELEASE OF DRIFTING BUOY
	1550	32 15.320N	133 24.850E	1100	A0402	ORI SIDE NET START
	1601	32 15.470N	133 24.910E	1098	A0402	ORI SIDE NET FINISH
	1712	32 25.190N	133 18.750E	953	A0302	CTD START
	1734	32 25.620N	133 19.450E	937	A0302	CTD DEEPEST
	1751	32 25.670N	133 19.850E	815	A0302	CTD FINISH
	1907	32 34.800N	133 12.640E	628	A0202	CTD START
	1922	32 34.700N	133 13.020E	651	A0202	CTD DEEPEST
	1934	32 34.780N	133 13.140E	663	A0202	CTD FINISH
	1939	32 34.800N	133 13.250E	664	A0202	RELEASE OF DRIFTING BUOY
	1944	32 34.690N	133 13.340E	679	A0202	ORI SIDE NET START
	1954	32 34.460N	133 13.460E	690	A0202	ORI SIDE NET FINISH
	2000	32 34.340N	133 13.550E	696		
	2036	32 40.150N	133 08.860E	281	A01A2	XBT
	2107	32 45.010N	133 06.030E	172	A0102	CTD-RMS START
	2117	32 44.960N	133 06.080E	190	A0102	CTD-RMS DEEPEST
	2130	32 44.850N	133 06.190E	276	A0102	CTD-RMS FINISH
	2218	32 47.870N	133 05.130E	237	S-1	GILL NET IN
94.03.01	0030	32 48.430N	133 05.480E	229	S-1	GILL NET OUT
	0126	32 48.680N	133 05.530E	229	S-1	FINISHED GILL NET OUT
	0222	32 48.040N	133 05.030E	228	G-1	CTD-RMS START
	0233	32 48.080N	133 05.160E	234	G-1	CTD-RMS DEEPEST
	0255	32 48.270N	133 05.150E	112	G-1	CTD-RMS FINISH
	0309	32 48.450N	133 05.110E	222	G-1	CHLTEC START
	0320	32 48.560N	133 05.090E	219	G-1	CHLTEC FINISHED
	0326	32 48.530N	133 05.150E	221	G-1	ORI SIDE NET START
	0337	32 48.190N	133 05.340E	229	G-1	ORI SIDE NET FINISH
	0354	32 48.290N	133 05.270E	228	G-1	MTD START
	0406	32 48.210N	133 05.390E	231	G-1	MTD START TO TOWING
	0420	32 48.020N	133 05.660E	237	G-1	MTD MESS CAST
	0428	32 47.970N	133 05.750E	240	G-1	MTD FINISH
	0547	32 35.730N	133 15.570E	790	G-2	XBT
	0550	32 35.000N	133 16.010E	780	G-2	XBT AGAIN
	0647	32 25.120N	133 25.410E	1002	G-3	CTD-RMS START
	0704	32 25.450N	133 26.020E	953	G-3	CTD-RMS DEEPEST
	0726	32 25.900N	133 26.610E	900	G-3	CTD-RMS FINISH
	0738	32 26.150N	133 27.260E	810	G-3	CHLTEC START
	0747	32 26.330N	133 27.760E	761	G-3	CHLTEC FINISH
	0751	32 26.390N	133 27.940E	764	G-3	ORI SIDE NET START
	0802	32 26.410N	133 28.250E	787	G-3	ORI SIDE NET FINISH
	0802	32 26.410N	133 28.250E	787	G-3	ORI SIDE NET FINISH
	0829	32 26.880N	133 28.970E	812	G-3	ORI NET START
	0836	32 27.340N	133 29.120E	817	G-3	ORI NET DEEPEST
	0843	32 27.830N	133 29.290E	838	G-3	ORI NET FINISH
	1129	32 40.810N	133 18.230E	715	GFD11	CTD START
	1138	32 40.750N	133 18.330E	719	GFD11	CTD DEEPEST

Y.M.D	JST	LAT.	LONG.	DEPTH	ST.NO.	COMENT
	1144	32 40.750N	133 18.410E	720	GFD11	CTD FINISH
	1150	32 40.820N	133 18.500E	721	GFD21	ORI NET START
	1204	32 41.230N	133 18.220E	685	GFD21	ORI NET FINISH
	1209	32 41.390N	133 18.100E	688	GFD31	ORI NET START (80 M)
	1213	32 41.550N	133 18.020E	679	GFD31	ORI NET DEEPEST
	1224	32 41.890N	133 17.820E	646	GFD31	ORI NET FINISH (80 M)
	1229	32 42.040N	133 17.710E	635	GFD41	ORI NET START (120 M)
	1232	32 42.130N	133 17.610E	628	GFD41	ORI NET DEEPEST
	1245	32 42.540N	133 17.310E	609	GFD41	ORI NET FINISH (120 M)
	1253	32 42.550N	133 17.220E	607	GFD51	ORI NET START (200 M)
	1303	32 42.310N	133 17.610E	628	GFD51	ORI NET FINISH (200 M)
	1313	32 42.060N	133 18.090E	642	GFD61	IKPT NET START
	1331	32 41.740N	133 18.880E	682	GFD61	IKPT NET FINISH
	1340	32 41.730N	133 18.950E	679	GFD71	MTD START
	1403	32 42.160N	133 19.000E	667	GFD71	MTD START TO TOWING
	1414	32 42.410N	133 18.880E	668	GFD71	MTD MESS CAST
	1427	32 42.700N	133 18.990E	659	GFD71	MTD FINISH
	1503	32 40.390N	133 20.830E	780		FRONT
	1527	32 38.970N	133 21.560E	6	GFD22	ORI NET START (40 M)
	1538	32 39.190N	133 22.400E	127	GFD22	ORI NET DEEPEST
	1538	32 39.190N	133 22.430E	107	GFD22	ORI NET FINISH (40 M)
	1541	32 39.230N	133 22.620E	301	GFD32	ORI NET START (80 M)
	1545	32 39.090N	133 22.860E	186	GFD32	ORI NET DEEPEST
	1557	32 39.440N	133 23.780E	293	GFD32	ORI NET FINISH (80 M)
	1600	32 39.490N	133 23.980E	284	GFD42	
	1603	32 39.540N	133 24.250E	354	GFD42	ORI NET START (120 M)
	1606	32 39.590N	133 24.490E	311	GFD42	ORI NET DEEPEST
	1620	32 39.770N	133 25.460E	359	GFD42	ORI NET FINISH (120M)
	1624	32 39.800N	133 25.760E	467	GFD52	ORI NET START
	1628	32 39.860N	133 26.020E	590	GFD52	ORI NET DEEPEST
	1633	32 39.910N	133 26.380E	836	GFD52	ORI NET FINISH
	1645	32 40.030N	133 27.130E	832	GFD62	IKPT NET START
	1652	32 40.100N	133 27.580E	832	GFD62	IKPT NET DEEPEST
	1659	32 40.170N	133 28.080E	832	GFD62	IKPT NET FINISH
	1700	32 40.180N	133 28.110E	831	GFD62	
	1710	32 40.330N	133 28.670E	827	GFD72	MTD START
	1723	32 40.510N	133 29.090E	822	GFD72	MTD START TO TOWING
	1733	32 40.860N	133 29.720E	831	GFD72	MTD MESS CAST
	1747	32 41.100N	133 30.280E	834	GFD72	MTD FINISH
	1748	32 41.120N	133 30.330E	835	GFD12	CTD-RMS START
	1759	32 41.240N	133 30.700E	839	GFD12	CTD-RMS DEEPEST
	1807	32 41.250N	133 30.770E	840	GFD12	CTD-RMS FINISH
	1902	32 39.490N	133 24.500E	836	GFN12	CTD-RMS START
	1913	32 39.530N	133 24.720E	838	GFN12	CTD-RMS DEEPEST
	1920	32 39.540N	133 24.810E	837	GFN12	CTD-RMS FINISH
	1928	32 39.550N	133 24.930E	840	GFN22	ORI NET START (40M)

Y.M.D	JST	LAT.	LONG.	DEPTH	ST.NO.	COMENT
	1929	32 39.550N	133 24.930E	839	GFN22	ORI NET DEEPEST
	1943	32 39.480N	133 24.930E	840	GFN22	ORI NET FINISH (40M)
	1945	32 39.460N	133 24.900E	840	GFN32	ORI NET START (80M)
	1948	32 39.450N	133 24.900E	840	GFN32	ORI NET DEEPEST
	2000	32 39.400N	133 24.800E	844	GFN32	
	2001	32 39.380N	133 24.790E	843	GFN32	ORI NET FINISH (80M)
	2006	32 39.340N	133 24.780E	843	GFN42	ORI NET START (120M)
	2010	32 39.350N	133 24.760E	842	GFN42	ORI NET DEEPEST (120M)
	2023	32 39.290N	133 24.740E	843	GFN42	ORI NET FINISH
	2028	32 39.250N	133 24.740E	844		ORI NET START
	2036	32 39.230N	133 24.720E	844	GFN52	ORI NET DEEPEST
	2040	32 39.190N	133 24.750E	845	GFN52	ORI NET FINISH
	2052	32 39.110N	133 24.710E	846	GFN62	IKPT NET START
	2102	32 39.070N	133 24.730E	848	GFN62	IKPT NET DEEPEST
	2110	32 39.030N	133 24.750E	848	GFN62	IKPT NET FINISH
	2120	32 39.170N	133 24.910E	846	GFN72	MTD START
	2142	32 39.780N	133 25.120E	837	GFN72	MTD START TO TOWING
	2151	32 40.130N	133 25.130E	823	GFN72	MTD MESS CAST
	2207	32 40.590N	133 25.210E	810	GFN72	MTD FINISH
	2307	32 40.730N	133 18.200E	724	GFN11	CTD START
	2316	32 40.720N	133 18.350E	721	GFN11	CTD DEEPEST
	2321	32 40.750N	133 18.440E	721	GFN11	CTD FINISH
	2328	32 40.710N	133 18.460E	724	GFN21	ORI NET START
	2330	32 40.710N	133 18.380E	721	GFN21	ORI NET DEEPEST (40M)
	2345	32 40.720N	133 18.050E	744	GFN21	ORI NET FINISH
	2347	32 40.710N	133 18.020E	745	GFN31	ORI NET START
	2349	32 40.690N	133 17.960E	783	GFN31	ORI NET DEEPEST (80M)
94.03.02	0000	32 40.660N	133 17.770E	723	GFN31	
	0003	32 40.680N	133 17.700E	691	GFN31	ORI NET FINISH
	0012	32 40.590N	133 17.490E	677	GFN41	ORI NET START (120 M)
	0020	32 40.560N	133 17.310E	677	GFN41	ORI NET DEEPEST
	0030	32 40.560N	133 17.080E	668	GFN41	ORI NET FINISH (120 M)
	0036	32 40.530N	133 16.940E	670	GFN51	ORI NET START (200 M)
	0047	32 40.480N	133 16.690E	664	GFN51	ORI NET FINISH (200 M)
	0056	32 40.450N	133 16.670E	664	GFN71	MTD START
	0138	32 40.640N	133 16.370E	658	GFN71	MTD START TO TOWING
	0150	32 40.660N	133 16.040E	637	GFN71	MTD MESS CAST
	0205	32 40.720N	133 15.960E	618	GFN71	MTD FINISH
	0211	32 40.650N	133 15.830E	621	GFN61	IKPT NET START
	0220	32 40.600N	133 15.550E	599	GFN61	IKPT NET DEEPEST
	0227	32 40.540N	133 15.350E	654	GFN61	IKPT NET FINISH
	0400	32 23.200N	133 27.730E	938		
	0448	32 13.030N	133 35.110E	1291	G-4	XBT
	0545	32 03.200N	133 45.530E	2960	G-5	CTD-RMS START
	0602	32 03.060N	133 45.990E	2679	G-5	CTD-RMS DEEPEST
	0613	32 03.180N	133 46.250E	3106	G-5	CTD-RMS FINISH

Y.M.D	JST	LAT.	LONG.	DEPTH	ST.NO.	COMENT
	0620	32 03.190N	133 46.450E	3125	G-5	CHLTEC START
	0630	32 03.150N	133 46.750E	3125	G-5	CHLTEC FINISH
	0635	32 03.030N	133 46.930E	3262	G-5	ORI SIDE NET START
	0647	32 02.510N	133 47.360E	3243	G-5	ORI SIDE NET FINISH
	0659	32 01.940N	133 47.780E	3251	G-5	ORI NET START
	0708	32 01.490N	133 48.050E	3292	G-5	ORI NET DEEPEST (300M)
	0719	32 01.170N	133 48.370E	3230	G-5	ORI NET FINISH
	0800	32 06.240N	133 51.260E	1635		
	0914	32 23.100N	134 00.050E	1695	G-6	CTD-RMS START
	0928	32 23.260N	134 00.380E	1701	G-6	CTD-RMS DEEPEST
	0945	32 23.430N	134 00.890E	1749	G-6	CTD-RMS FINISH
	0952	32 23.480N	134 01.280E	1759	G-6	CHLTEC START
	1001	32 23.590N	134 01.530E	1757	G-6	CHLTEC FINISH
	1010	32 23.700N	134 01.850E	1802	G-6	ORI NET START (300M)
	1018	32 23.820N	134 02.340E	1800	G-6	ORI NET DEEPEST (300M)
	1025	32 23.900N	134 02.800E	1799	G-6	ORI NET FINISH
	1032	32 24.190N	134 03.010E	1807	G-6	ORI SIDE NET START
	1042	32 24.660N	134 02.860E	1801	G-6	ORI SIDE NET FINISH
	1154	32 35.060N	133 50.020E	1135	G-7	XBT
	1200	32 36.320N	133 48.950E	1064		
	1258	32 47.180N	133 40.990E	1041	G-8	CTD-RMS START
	1315	32 47.410N	133 41.440E	1043	G-8	CTD-RMS DEEPEST
	1340	32 47.780N	133 41.980E	1045	G-8	CTD-RMS FINISH
	1344	32 47.830N	133 42.120E	1045	G-8	CHLTEC START
	1355	32 48.130N	133 42.400E	1046	G-8	CHLTEC FINISH
	1403	32 48.370N	133 42.500E	1048	G-8	ORI SIDE NET START
	1414	32 48.740N	133 42.450E	1047	G-8	ORI SIDE NET FINISH
	1539	32 59.490N	133 30.370E	489	G-9	XBT
	1600	33 01.610N	133 28.660E	387		
	1807	33 00.780N	133 28.060E	376	S-2	GILL NET IN
	2110	32 58.510N	133 27.660E	376	S-2	GILL NET OUT
	2138	32 57.780N	133 27.590E	376	S-3	GILL NET IN
	2320	32 56.700N	133 27.300E	376	S-3	GILL NET OUT
	2342	32 56.070N	133 27.250E	376	S-4	GILL NET IN
94.03.03	0000	32 55.770N	133 27.130E	376	S-4	
	0154	32 54.720N	133 27.100E	376	S-4	GILL NET OUT
	0206	32 54.580N	133 27.110E	376	G-9-S	CTD-RMS START
	0215	32 54.540N	133 27.120E	376	G-9-S	CTD-RMS DEEPEST
	0230	32 54.450N	133 27.120E	376	G-9-S	CTD-RMS FINISH
	0238	32 54.380N	133 27.070E	376	G-9-S	MTD START
	0251	32 54.350N	133 27.200E	376	G-9-S	MTD START TO TOWING
	0306	32 54.520N	133 27.580E	376	G-9-S	MTD MESS CAST
	0319	32 54.550N	133 27.790E	376	G-9-S	MTD FINISH
	0400	33 00.580N	133 26.260E	376		
	0450	33 11.140N	133 22.060E	112	G-10	CTD-RMS START
	0457	33 11.140N	133 22.130E	106	G-10	CTD-RMS DEEPEST

Y.M.D	JST	LAT.	LONG.	DEPTH	ST.NO.	COMENT
	0502	33 11.170N	133 22.160E	107	G-10	CTD-RMS FINISH
	0506	33 11.160N	133 22.230E	108	G-10	CHLTEC START
	0516	33 11.170N	133 22.270E	109	G-10	CHLTEC FINISH
	0520	33 11.190N	133 22.220E	112	G-10	ORI SIDE NET START
	0531	33 11.340N	133 21.910E	108	G-10	ORI SIDE NET FINISH
	0600	33 13.270N	133 26.480E	116		
	0745	33 23.360N	133 49.290E	101	G-11	CTD-RMS START
	0754	33 23.370N	133 49.080E	101	G-11	CTD-RMS DEEPEST
	0802	33 23.390N	133 48.940E	102	G-11	CTD-RMS FINISH
	0820	33 23.380N	133 48.660E	102	G-11	CTD-RMS START
	0827	33 23.390N	133 48.590E	102	G-11	CTD-RMS DEEPEST
	0841	33 23.360N	133 48.360E	102	G-11	CTD-RMS FINISH
	0845	33 23.360N	133 48.300E	66	G-11	CHLTEC START
	0856	33 23.320N	133 48.110E	207	G-11	CHLTEC FINISH
	0901	33 23.240N	133 48.170E	203	G-11	ORI SIDE NET START
	0906	33 23.180N	133 48.300E	213	G-11	ORI SIDE NET FINISH
	1041	33 14.100N	133 56.870E	660	G-12	XBT
	1145	33 03.320N	134 07.180E	679	G-13	CTD-RMS START
	1200	33 03.470N	134 07.250E	671	G-13	CTD-RMS DEEPEST
	1223	33 03.740N	134 07.360E	663	G-13	CTD-RMS FINISH
	1227	33 03.760N	134 07.360E	659	G-13	CHLTEC START
	1236	33 03.870N	134 07.370E	653	G-13	CHLTEC FINISH
	1241	33 04.020N	134 07.440E	647	G-13	ORI SIDE NET START
	1247	33 04.300N	134 07.640E	624	G-13	ORI SIDE NET FINISH
	1401	32 51.900N	134 17.120E	1105	G-14	XBT
	1600	33 17.010N	133 55.190E	512		
	1825	33 23.770N	133 49.280E	94	S-5	GILL NET IN
	2102	33 24.860N	133 48.980E	81	S-5	GILL NET OUT
	2129	33 22.880N	133 48.780E	109	S-6	GILL NET IN
	2346	33 23.300N	133 48.080E	103	S-6	GILL NET OUT
94.03.04	0000	33 23.240N	133 48.030E	104	S-6	
	0013	33 23.230N	133 48.070E	104	S-6	MTD START TO TOWING
	0028	33 23.280N	133 48.480E	103	S-6	MTD MESS CAST
	0037	33 23.230N	133 48.630E	103	S-6	MTD FINISH
	0043	33 23.120N	133 48.620E	105	S-6	ORI SIDE NET START
	0048	33 22.940N	133 48.610E	108	S-6	ORI SIDE NET FINISH
	0108	33 21.660N	133 48.430E	130	S-6	RELEASE OF DRIFTING BUOY
	0400	33 08.110N	134 34.030E	51		
	0800	33 03.370N	135 59.180E	74		
	1200	33 18.190N	136 59.810E	2844		
	1600	33 06.060N	137 11.990E	1631		
	2000	33 10.370N	137 30.110E	3939		
94.03.05	0000	33 29.390N	137 59.960E	2214		
	0400	33 03.910N	138 18.480E	2493		
	0800	33 19.990N	138 17.560E	3992		
	0948	33 11.330N	137 55.870E	3698	K-21	CTD-RMS START

Y.M.D	JST	LAT.	LONG.	DEPTH	ST.NO.	COMENT
	1004	33 11.650N	137 56.620E	3644	K-21	CTD-RMS DEEPEST
	1033	33 12.110N	137 57.950E	3621	K-21	CTD-RMS FINISH
	1040	33 12.210N	137 58.280E	3632	K-21	ORI SIDE NET START
	1045	33 12.250N	137 58.400E	3637	K-21	ORI SIDE NET FINISH
	1055	33 12.390N	137 58.740E	3653	K-21	IKPT NET START
	1102	33 12.440N	137 58.930E	3663	K-21	IKPT NET DEEPEST
	1109	33 12.480N	137 59.140E	3676	K-21	IKPT NET FINISH
	1113	33 12.610N	137 59.340E	3674	K-21	MTD START
	1135	33 13.290N	138 00.100E	3659	K-21	MTD START TO TOWING
	1151	33 14.060N	138 00.380E	3352	K-21	MTD MESS CAST
	1200	33 14.390N	138 00.640E	3366	K-21	
	1200	33 14.400N	138 00.660E	3376	K-21	MTD FINISH
	1223	33 16.180N	138 00.180E	3272	K-22	CTD-RMS START
	1238	33 16.670N	138 00.820E	3401	K-22	CTD-RMS DEEPEST
	1253	33 17.050N	138 01.350E	3448	K-22	CTD-RMS FINISH
	1259	33 17.350N	138 01.640E	3417	K-22	ORI SIDE NET START
	1305	33 17.723N	138 01.745E	3370	K-22	ORI SIDE NET FINISH
	1337	33 21.260N	138 00.100E	3361	K-23	CTD-RMS START
	1354	33 21.830N	138 00.780E	3278	K-23	CTD-RMS DEEPEST
	1411	33 22.410N	138 01.410E	3153	K-23	CTD-RMS FINISH
	1416	33 22.800N	138 01.590E	3049	K-23	ORI SIDE NET START
	1422	33 23.240N	138 01.670E	2986	K-23	ORI SIDE NET FINISH
	1427	33 23.530N	138 01.790E	3205	K-23	MTD START
	1442	33 24.360N	138 02.310E	3377	K-23	MTD START TO TOWING
	1457	33 25.280N	138 02.730E	2822	K-23	MTD MESS CAST
	1511	33 26.050N	138 03.320E	3207	K-23	MTD FINISH
	1517	33 26.330N	138 03.490E	3322	K-23	IKPT NET START
	1530	33 26.770N	138 03.500E	3523	K-23	IKPT NET DEEPEST
	1600	33 25.740N	138 00.460E	2035		
	1611	33 25.610N	137 59.800E	1962	K-24	CTD-RMS START
	1626	33 25.750N	138 00.150E	2041	K-24	CTD-RMS DEEPEST
	1640	33 25.890N	138 00.400E	2085	K-24	CTD-RMS FINISH
	1644	33 26.070N	138 00.500E	2224	K-24	ORI SIDE NET START
	1653	33 26.390N	138 00.550E	2335	K-24	ORI SIDE NET FINISH
	1655	33 26.460N	138 00.540E	2197	K-24	IKPT NET START
	1701	33 26.710N	138 00.540E	2283	K-24	IKPT NET DEEPEST
	1707	33 26.900N	138 00.530E	2698	K-24	IKPT NET FINISH
	1729	33 27.350N	138 00.760E	3021	K-24	MTD START TO TOWING
	1743	33 27.740N	138 00.850E	3332	K-24	MTD MESS CAST
	1754	33 28.020N	138 00.950E	3313	K-24	MTD FINISH
	1835	33 31.020N	138 00.070E	3177	K-25	CTD-RMS START
	1847	33 30.980N	138 00.260E	3165	K-25	CTD-RMS DEEPEST
	1906	33 30.930N	138 00.540E	3079	K-25	CTD-RMS FINISH
	1910	33 30.830N	138 00.550E	3011	K-25	ORI SIDE NET START
	1915	33 30.900N	138 00.460E	3160	K-25	ORI SIDE NET FINISH
	2000	33 35.970N	137 59.970E	3964	K-26	CTD-RMS START

Y.M.D	JST	LAT.	LONG.	DEPTH	ST.NO.	COMENT
	2019	33 35.770N	138 00.250E	3969	K-26	CTD-RMS DEEPEST
	2034	33 35.660N	138 00.540E	3949	K-26	CTD-RMS FINISH
	2038	33 35.620N	138 00.640E	3949	K-26	ORI SIDE NET START
	2044	33 35.510N	138 00.560E	3946	K-26	ORI SIDE NET FINISH
	2105	33 35.630N	138 00.620E	3950	K-26	MTD START TO TOWING
	2122	33 35.970N	138 00.390E	3959	K-26	MTD MESS CAST
	2135	33 36.090N	138 00.450E	3954	K-26	MTD FINISH
	2216	33 40.670N	138 00.060E	3857	K-27	CTD-RMS START
	2234	33 40.430N	138 00.310E	3920	K-27	CTD-RMS DEEPEST
	2252	33 40.260N	138 00.280E	3912	K-27	CTD-RMS FINISH
	2256	33 40.260N	138 00.190E	3915	K-27	ORI SIDE NET START
	2301	33 40.360N	138 00.070E	3934	K-27	ORI SIDE NET FINISH
	2355	33 45.970N	138 00.030E	3648	K-28	CTD-RMS START
94.03.06	0009	33 45.800N	137 59.970E	3735	K-28	CTD-RMS DEEPEST
	0028	33 45.800N	137 59.910E	3746	K-28	CTD-RMS FINISH
	0058	33 45.990N	137 59.750E	3713	K-28	MTD START TO TOWING
	0114	33 46.350N	137 59.480E	3691	K-28	MTD MESS CAST
	0128	33 46.520N	137 59.480E	3686	K-28	MTD FINISH
	0248	33 50.740N	138 00.100E	3134	K-29	CTD-RMS START
	0303	33 50.670N	138 00.080E	3131	K-29	CTD-RMS DEEPEST
	0321	33 50.560N	138 00.090E	3270	K-29	CTD-RMS FINISH
	0400	33 53.160N	138 00.250E	2875		
	0435	33 55.940N	137 59.910E	2518	K-30	CTD-RMS START
	0450	33 55.630N	137 59.800E	2903	K-30	CTD-RMS DEEPEST
	0512	33 55.200N	137 59.560E	2108	K-30	CTD-RMS FINISH
	0648	34 00.780N	137 59.790E	3766	K-31	CTD-RMS START
	0702	34 00.570N	137 59.810E	4137	K-31	CTD-RMS DEEPEST
	0725	34 00.130N	137 59.360E	2887	K-31	CTD-RMS FINISH
	0725	34 00.130N	137 59.360E	2887	K-31	CTD-RMS FINISH
	0800	34 02.440N	137 59.770E	1608		
	0947	34 10.900N	138 00.060E	850	K-32	CTD-RMS START
	1003	34 10.830N	138 00.060E	850	K-32	CTD-RMS DEEPEST
	1021	34 10.690N	138 00.110E	846	K-32	CTD-RMS FINISH
	1200	34 19.280N	137 59.200E	692		
	1217	34 20.910N	137 59.920E	534	K-33	CTD-RMS START
	1238	34 21.030N	137 59.840E	525	K-33	CTD-RMS DEEPEST
	1254	34 20.960N	137 59.820E	533	K-33	CTD-RMS FINISH
	1519	34 09.850N	137 29.850E	1333	KX-1	XBT
	1555	33 59.760N	137 30.000E	1726	KX-2	XBT
	1600	33 58.520N	137 30.000E	1699		
	1631	33 49.810N	137 30.530E	1860	KX-3	XBT
	1705	33 39.800N	137 30.070E	3360	KX-4	XBT
	1740	33 30.000N	137 30.030E	3967	KX-5	XBT
	1800	33 24.690N	137 30.100E	3859		
	1817	33 19.870N	137 30.110E	3913	KX-6	XBT
	1852	33 09.980N	137 30.100E	3932	KX-7	XBT

Y.M.D	JST	LAT.	LONG.	DEPTH	ST.NO.	COMENT
	1928	33 00.000N	137 30.040E	3485	KX-8	XBT
	2000	33 02.280N	137 39.370E	3135		
	2255	33 16.900N	138 30.110E	250	K-34	CTD START
	2314	33 17.330N	138 30.840E	3097	K-34	CTD DEEPEST
	2325	33 17.550N	138 31.260E	3715	K-34	CTD FINISH
	2329	33 17.620N	138 31.370E	3694	K-34	ORI SIDE NET START
	2335	33 17.720N	138 31.380E	2950	K-34	ORI SIDE NET FINISH
	2340	33 18.140N	138 31.440E	2903	K-34	IKPT NET START
	2347	33 18.500N	138 31.780E	2131	K-34	IKPT NET DEEPEST
	2352	33 18.760N	138 31.950E	2212	K-34	IKPT NET FINISH
94.03.07	0000	33 19.160N	138 32.290E	1880		s/co on 241°
	0051	33 30.200N	138 30.220E	3498	K-35	CTD-RMS START
	0105	33 30.470N	138 30.420E	3489	K-35	CTD DEEPEST
	0113	33 30.640N	138 30.480E	3484	K-35	CTD FINISH
	0120	33 30.850N	138 30.640E	3465	K-35	ORI SIDE NET START
	0126	33 31.190N	138 30.650E	3436	K-35	ORI SIDE NET FINISH
	0132	33 31.580N	138 30.590E	3419	K-35	IKPT NET START
	0139	33 31.990N	138 30.590E	3415	K-35	IKPT NET DEEPEST
	0144	33 32.250N	138 30.630E	3415	K-35	IKPT NET FINISH
	0233	33 40.160N	138 30.140E	2388	K-36	CTD START
	0246	33 40.430N	138 30.260E	2372	K-36	CTD DEEPEST
	0255	33 40.690N	138 30.260E	2346	K-36	CTD FINISH
	0300	33 40.850N	138 30.370E	2222	K-36	ORI SIDE NET START
	0305	33 41.200N	138 30.400E	2165	K-36	ORI SIDE NET FINISH
	0400	33 53.760N	138 29.990E	3448		
	0411	33 55.350N	138 30.010E	3532	K-37	CTD-RMS START
	0424	33 55.750N	138 30.250E	3520	K-37	CTD DEEPEST
	0435	33 55.950N	138 30.390E	3505	K-37	CTD FINISH
	0438	33 56.000N	138 30.410E	3606	K-37	ORI SIDE NET START
	0444	33 56.050N	138 30.430E	3541	K-37	ORI SIDE NET FINISH
	0448	33 56.050N	138 30.420E	3594	K-37	IKPT NET START
	0457	33 56.140N	138 30.460E	3579	K-37	IKPT NET DEEPEST
	0502	33 56.170N	138 30.440E	3527	K-37	IKPT NET FINISH
	0607	34 10.390N	138 29.870E	3633	K-38	CTD START
	0619	34 10.700N	138 29.670E	3628	K-38	CTD DEEPEST
	0631	34 10.890N	138 29.580E	3625	K-38	CTD FINISH
	0635	34 11.060N	138 29.470E	3622	K-38	ORI SIDE NET START
	0641	34 11.400N	138 29.240E	3621	K-38	ORI SIDE NET FINISH
	0645	34 11.610N	138 29.140E	3613	K-38	IKPT NET START
	0655	34 12.090N	138 28.740E	3604	K-38	IKPT NET DEEPEST
	0701	34 12.360N	138 28.460E	3597	K-38	LOST IKPT NET
	0800	34 20.110N	138 41.030E	3611		
	1113	34 48.180N	139 26.950E	854	KS-1	LAUNCH OF ADCP1
	1129	34 48.290N	139 26.380E	815	KS-1	FINISH TO LAUNCH OF ADCP1
	1146	34 48.300N	139 26.500E	839	KS-2	LAUNCH OF ADCP2
	1210	34 48.450N	139 25.650E	818	KS-2	FINISH TO LAUNCH OF ADCP2

Y.M.D	JST	LAT.	LONG.	DEPTH	ST.NO.	COMENT
	1313	34 49.340N	139 25.650E	756	KS-2	COM'CED HEAVE UP ADCP
	1317	34 49.430N	139 25.580E	810	KS-2	START TO RETREIVE OF ADCP
	1346	34 49.880N	139 25.590E	1009	KS-2	FINISH TO RETREIVE OF ADCP
	1351	34 49.980N	139 25.520E	1013	KS-2	CTD START
	1404	34 50.190N	139 25.420E	1000	KS-2	CTD-RMS DEEPEST
	1422	34 50.380N	139 25.240E	1066	KS-2	CTD-RMS FINISH
	1444	34 50.720N	139 25.390E	1226	KS-2	MTD START TO TOWING
	1449	34 50.870N	139 25.480E	1285	KS-2	MTD MESS CAST
	1459	34 50.960N	139 25.650E	1318	KS-2	MTD FINISH
	1600	34 59.850N	139 37.910E	2007		
	1800	35 25.140N	139 43.020E	38		
	1815	35 26.230N	139 43.320E	33		LET'GO ANCHOR

Leg 2:Set Sail from Yokohama to Tokyo

94.03.12	1400	35 26.630N	139 39.420E	3		
	1600	35 08.760N	139 44.550E	429		
	2000	35 10.540N	139 17.420E	974		
94.03.13	0000	35 10.300N	139 16.180E	1215		
	0400	35 11.910N	139 19.780E	1033		
	0718	34 55.840N	139 29.710E	1260	KS-2	XBT
	0728	34 53.200N	139 29.860E	1587	KS-3	XBT
	0736	34 50.880N	139 29.850E	1733	KS-4	XBT
	0800	34 48.080N	139 29.470E	1589		
	0801	34 48.070N	139 29.470E	1669	KS-5	CTD-RMS START
	0818	34 48.080N	139 29.500E	1428	KS-5	CTD-RMS DEEPEST
	0840	34 48.070N	139 29.220E	1490	KS-5	CTD-RMS FINISH
	0902	34 48.030N	139 29.180E	1500	KS-5	MTD START TO TOWING
	0908	34 48.190N	139 29.350E	1439	KS-5	MTD MESS CAST
	0918	34 48.210N	139 29.520E	1450	KS-5	MTD FINISH
	0941	34 45.800N	139 29.650E	1087	KS-6	XBT
	0950	34 43.410N	139 29.660E	993	KS-7	XBT
	1000	34 40.790N	139 29.610E	726	KS-8	XBT
	1200	34 31.390N	138 55.780E	290		
	1600	34 24.080N	137 39.730E	1101		
	1810	34 19.690N	137 00.000E	73	K-39	XBT
	1817	34 19.290N	136 59.990E	78	K-39	ORI SIDE NET START
	1822	34 19.160N	137 00.020E	82	K-39	ORI SIDE NET FINISH
	1901	34 10.000N	137 00.130E	1349	K-40	XBT
	1939	33 59.970N	136 59.960E	1131	K-41	XBT
	1945	33 59.480N	136 59.990E	1103	K-41	ORI SIDE NET START
	1949	33 59.330N	136 59.960E	1103	K-41	ORI SIDE NET FINISH
	2000	33 57.820N	137 00.020E	1260		RUNG UP ENGINES
	2028	33 50.000N	136 59.950E	2026	K-42	XBT
	2101	33 41.040N	136 59.670E	2011	K-43	XBT
	2109	33 40.020N	136 59.900E	2020	K-43	ORI SIDE NET START

Y.M.D	JST	LAT.	LONG.	DEPTH	ST.NO.	COMENT
	2112	33 39.900N	136 59.950E	2020	K-43	ORI SIDE NET FINISH
	2153	33 30.130N	137 00.050E	2062	K-44	XBT
	2230	33 19.950N	137 00.090E	2687	K-45	XBT
	2308	33 10.060N	137 00.190E	4052	K-46	XBT
	2347	33 00.110N	137 00.080E	5897	K-47	XBT
94.03.14	0000	32 59.410N	137 04.000E	6672		
	0109	33 00.040N	137 30.230E	3952	K-48	XBT
	0154	33 10.110N	137 29.870E	3939	K-49	XBT
	0233	33 19.960N	137 29.830E	3945	K-50	XBT
	0313	33 30.010N	137 29.890E	3962	K-51	XBT
	0353	33 40.030N	137 29.910E	5511	K-52	XBT
	0400	33 41.690N	137 29.820E	3146		
	0433	33 50.010N	137 29.910E	3023	K-53	XBT
	0513	34 00.000N	137 29.950E	3450	K-54	XBT
	0552	34 10.000N	137 30.010E	4845	K-55	XBT
	0631	34 20.030N	137 30.000E	5593	K-56	XBT
	0708	34 29.840N	137 30.020E	195	K-57	PASSED K-57
	0800	34 30.060N	137 46.790E	618		
	0857	34 30.040N	138 00.190E	505	K-58	CTD-RMS START
	0915	34 30.020N	138 00.500E	492	K-58	CTD-RMS DEEPEST
	0937	34 29.850N	138 00.810E	484	K-58	CTD-RMS FINISH
	0942	34 29.780N	138 00.790E	486	K-58	ORI SIDE NET START
	0946	34 29.700N	138 00.640E	492	K-58	ORI SIDE NET FINISH
	0951	34 29.610N	138 00.570E	496	K-58	ORI NET START
	0958	34 29.470N	138 00.340E	508	K-58	ORI NET DEEPEST
	1005	34 29.340N	138 00.110E	520	K-58	ORI NET FINISH
	1023	34 29.310N	137 59.990E	525	K-58	MTD START TO TOWING
	1034	34 29.400N	137 59.720E	539	K-58	MTD MESS CAST
	1043	34 29.420N	137 59.660E	543	K-58	MTD FINISH
	1122	34 24.850N	137 59.970E	449	K-59	CTD-RMS START
	1142	34 24.740N	138 00.050E	447	K-59	CTD-RMS DEEPEST
	1201	34 24.620N	138 00.050E	447	K-59	CTD-RMS FINISH
	1205	34 24.560N	137 59.900E	452	K-59	ORI SIDE NET START
	1208	34 24.500N	137 59.730E	454	K-59	ORI SIDE NET FINISH
	1248	34 20.040N	138 00.050E	596	K-60	CTD-RMS START
	1309	34 19.850N	137 59.900E	617	K-60	CTD-RMS DEEPEST
	1327	34 19.760N	137 59.810E	639	K-60	CTD-RMS FINISH
	1331	34 19.710N	137 59.690E	651	K-60	ORI SIDE NET START
	1335	34 19.610N	137 59.530E	659	K-60	ORI SIDE NET FINISH
	1415	34 15.010N	137 59.830E	895	K-61	CTD-RMS START
	1436	34 14.820N	137 59.520E	870	K-61	CTD-RMS DEEPEST
	1452	34 14.670N	137 59.180E	854	K-61	CTD-RMS FINISH
	1456	34 14.640N	137 58.990E	839	K-61	ORI SIDE NET START
	1501	34 14.570N	137 58.610E	818	K-61	ORI SIDE NET FINISH
	1542	34 10.000N	137 59.970E	928	K-62	CTD-RMS START
	1604	34 09.770N	137 59.520E	903	K-62	CTD-RMS DEEPEST

Y.M.D	JST	LAT.	LONG.	DEPTH	ST.NO.	COMENT
	1624	34 09.490N	137 59.240E	898	K-62	CTD-RMS FINISH
	1629	34 09.450N	137 59.160E	904	K-62	ORI SIDE NET START
	1636	34 09.500N	137 58.800E	875	K-62	ORI SIDE NET FINISH
	1656	34 09.440N	137 58.220E	850	K-62	MTD START TO TOWING
	1711	34 09.670N	137 57.530E	838	K-62	MTD MESS CAST
	1725	34 09.650N	137 57.140E	847	K-62	MTD FINISH
	1728	34 09.620N	137 57.000E	853	K-62	ORI NET START
	1735	34 09.710N	137 56.640E	855	K-62	ORI NET DEEPEST
	1742	34 09.770N	137 56.350E	806	K-62	ORI NET FINISH
	1840	34 04.970N	137 59.910E	1270	K-63	ORI SIDE NET START
	1847	34 05.050N	137 59.620E	1189	K-63	ORI SIDE NET FINISH
	1851	34 05.060N	137 59.470E	1163	K-63	CTD-RMS START
	1913	34 04.980N	137 58.910E	1204	K-63	CTD-RMS DEEPEST
	1938	34 04.820N	137 58.310E	1284	K-63	CTD-RMS FINISH
	2000	34 02.330N	137 59.120E	1566		
	2024	33 59.850N	138 00.120E	1526	K-64	CTD-RMS START
	2048	33 59.330N	138 00.340E	1610	K-64	CTD-RMS DEEPEST
	2110	33 58.930N	138 00.240E	1599	K-64	CTD-RMS FINISH
	2114	33 58.880N	138 00.180E	1611	K-64	ORI SIDE NET START
	2117	33 58.890N	138 00.060E	1626	K-64	ORI SIDE NET FINISH
	2150	33 55.030N	137 59.880E	2715	K-65	ORI SIDE NET START
	2154	33 55.000N	137 59.760E	2640	K-65	ORI SIDE NET FINISH
	2159	33 54.910N	137 59.750E	2874	K-65	CTD-RMS START
	2225	33 54.460N	137 59.810E	3371	K-65	CTD-RMS DEEPEST
	2242	33 54.310N	137 59.630E	2700	K-65	CTD-RMS FINISH
	2323	33 49.850N	137 59.970E	3536	K-66	CTD-RMS START
	2345	33 49.430N	138 00.040E	3422	K-66	CTD-RMS DEEPEST
94.03.15	0004	33 49.060N	138 00.100E	3443	K-66	CTD-RMS FINISH
	0008	33 49.090N	138 00.090E	3431	K-66	ORI SIDE NET START
	0011	33 49.170N	138 00.060E	3452	K-66	ORI SIDE NET FINISH
	0033	33 49.230N	138 00.010E	3412	K-66	MTD START TO TOWING
	0039	33 49.370N	137 59.930E	3406	K-66	MTD MESS CAST
	0052	33 49.390N	137 59.920E	3413	K-66	MTD FINISH
	0132	33 45.050N	138 00.020E	3720	K-67	CTD-RMS START
	0152	33 45.040N	138 00.010E	3717	K-67	CTD-RMS DEEPEST
	0211	33 44.970N	138 00.080E	3715	K-67	CTD-RMS FINISH
	0214	33 45.060N	138 00.020E	3715	K-67	ORI SIDE NET START
	0216	33 45.130N	137 59.970E	3718	K-67	ORI SIDE NET FINISH
	0301	33 40.100N	138 00.120E	3876		CTD-RMS START
	0320	33 40.190N	138 00.250E	3911	K-68	CTD-RMS DEEPEST
	0338	33 40.290N	138 00.410E	3915	K-68	CTD-RMS FINISH
	0341	33 40.390N	138 00.400E	3913	K-68	ORI SIDE NET START
	0343	33 40.470N	138 00.410E	3874	K-68	ORI SIDE NET FINISH
	0400	33 39.050N	138 00.250E	3944		
	0434	33 35.000N	138 00.010E	3927	K-69	ORI SIDE NET START
	0438	33 35.210N	138 00.020E	3929	K-69	ORI SIDE NET FINISH

Y.M.D	JST	LAT.	LONG.	DEPTH	ST.NO.	COMENT
	0443	33 35.350N	138 00.100E	3935	K-69	CTD-RMS START
	0506	33 35.640N	138 00.480E	3953	K-69	CTD-RMS DEEPEST
	0506	33 35.640N	138 00.480E	3953	K-69	CTD-RMS DEEPEST
	0523	33 35.670N	138 00.820E	3942	K-69	CTD-RMS FINISH
	0621	33 29.930N	137 59.840E	2967	K-70	CTD-RMS START
	0640	33 30.040N	137 59.980E	2945	K-70	CTD-RMS DEEPEST
	0656	33 29.940N	138 00.180E	2883	K-70	CTD-RMS FINISH
	0659	33 29.980N	138 00.260E	2853	K-70	ORI SIDE NET START
	0703	33 30.110N	138 00.230E	2872	K-70	ORI SIDE NET FINISH
	0721	33 30.570N	138 00.280E	2947	K-70	MTD START TO TOWING
	0731	33 30.960N	138 00.230E	3168	K-70	MTD MESS CAST
	0742	33 31.270N	138 00.400E	3337	K-70	MTD FINISH
	0800	33 29.860N	138 00.400E	2808		
	0841	33 25.110N	138 00.040E	1904	K-71	ORI SIDE NET START
	0844	33 25.190N	138 00.000E	1909	K-71	ORI SIDE NET FINISH
	0848	33 25.210N	137 59.940E	1918	K-71	CTD-RMS START
	0906	33 25.140N	138 00.250E	1832	K-71	CTD-RMS DEEPEST
	0932	33 25.080N	138 00.810E	1881	K-71	CTD-RMS FINISH
	1020	33 20.030N	138 00.200E	3500	K-72	CTD-RMS START
	1047	33 19.890N	138 01.210E	3502	K-72	CTD-RMS DEEPEST
	1108	33 19.760N	138 01.760E	3472	K-72	CTD-RMS FINISH
	1111	33 19.750N	138 01.840E	3468	K-72	ORI SIDE NET START
	1115	33 19.750N	138 01.880E	3469	K-72	ORI SIDE NET FINISH
	1204	33 15.030N	138 00.400E	3391	K-73	ORI SIDE NET START
	1208	33 15.190N	138 00.600E	3263	K-73	ORI SIDE NET FINISH
	1213	33 15.250N	138 00.890E	3297	K-73	CTD-RMS START
	1233	33 15.140N	138 01.970E	3535	K-73	CTD-RMS DEEPEST
	1253	33 14.980N	138 02.840E	3926	K-73	CTD-RMS FINISH
	1356	33 10.130N	138 00.230E	4050	K-74	CTD-RMS DEEPEST
	1417	33 09.890N	138 01.390E	3826	K-74	CTD-RMS DEEPEST
	1435	33 09.750N	138 02.260E	3965	K-74	CTD-RMS FINISH
	1439	33 09.810N	138 02.500E	3980	K-74	ORI SIDE NET START
	1442	33 09.920N	138 02.700E	3977	K-74	ORI SIDE NET FINISH
	1459	33 10.110N	138 03.710E	3880	K-74	MTD START TO TOWING
	1509	33 10.310N	138 04.140E	3816	K-74	MTD MESS CAST
	1521	33 10.380N	138 04.910E	3862	K-74	MTD FINISH
	1646	33 10.120N	138 30.330E	3245	K-78	CTD START
	1709	33 10.270N	138 31.470E	3160	K-78	CTD-RMS DEEPEST
	1718	33 10.270N	138 31.830E	3115	K-78	CTD FINISH
	1829	33 19.950N	138 30.440E	2321	K-79	CTD START
	1852	33 19.820N	138 31.270E	3392	K-79	CTD-RMS DEEPEST
	1904	33 19.860N	138 31.620E	3393	K-79	CTD-RMS FINISH
	2000	33 27.980N	138 30.450E	4053		
	2020	33 29.900N	138 29.850E	5464	K-80	XBT
	2143	33 39.970N	138 29.930E	4441	K-81	XBT
	2255	33 49.960N	138 29.840E	6219	K-82	XBT

Y.M.D	JST	LAT.	LONG.	DEPTH	ST.NO.	COMENT
94.03.16	0000	33 59.360N	138 30.030E	3615		
	0015	34 00.010N	138 30.130E	3582	K-83	CTD START
	0032	34 00.220N	138 30.360E	3576	K-83	CTD DEEPEST
	0050	34 00.460N	138 30.490E	3571	K-83	CTD FINISH
	0149	34 10.110N	138 29.810E	3637	K-84	CTD START
	0208	34 10.340N	138 29.710E	3634	K-84	CTD DEEPEST
	0221	34 10.480N	138 29.740E	3632	K-84	CTD FINISH
	0319	34 20.010N	138 29.890E	2720	K-85	CTD START
	0339	34 19.930N	138 29.660E	2773	K-85	CTD DEEPEST
	0349	34 19.940N	138 29.720E	2765	K-85	CTD FINISH
	0400	34 19.950N	138 29.520E	2775		
	0452	34 30.050N	138 30.130E	2259	K-86	CTD START
	0513	34 30.390N	138 30.180E	2073	K-86	CTD DEEPEST
	0524	34 30.600N	138 30.170E	2026	K-86	CTD FINISH
	0718	34 07.970N	138 34.190E	3628	G-16	CTD START
	0737	34 08.250N	138 34.130E	3537	G-16	CTD-RMS DEEPEST
	0748	34 08.460N	138 34.140E	3565	G-16	CTD-RMS FINISH
	0756	34 08.610N	138 34.150E	3603	G-16	ORI SIDE NET START
	0759	34 08.800N	138 34.310E	3593	G-16	ORI SIDE NET FINISH
	0800	34 08.810N	138 34.320E	3593	G-16	
	0807	34 09.020N	138 34.370E	3498	G-16	CHLTEC START
	0814	34 09.150N	138 34.400E	3514	G-16	CHLTEC FINISH
	0819	34 09.310N	138 34.510E	3595	G-16	ORI NET START
	0827	34 09.640N	138 34.800E	3559	G-16	ORI NET DEEPEST
	0834	34 09.860N	138 34.870E	3443	G-16	ORI NET FINISH
	1008	33 56.040N	138 45.890E	77	G-17	ORI SIDE NET START
	1011	33 56.060N	138 45.820E	81	G-17	ORI SIDE NET FINISH
	1016	33 56.100N	138 45.850E	78	G-17	CTD-RMS START
	1031	33 56.130N	138 45.840E	78	G-17	CTD-RMS DEEPEST
	1036	33 56.140N	138 45.880E	154	G-17	CTD-RMS FINISH
	1042	33 56.140N	138 45.910E	75	G-17	CHLTEC START
	1047	33 56.170N	138 45.930E	76	G-17	CHLTEC FINISH
	1052	33 56.140N	138 45.940E	75	G-17	ORI NET START
	1055	33 56.160N	138 45.880E	75	G-17	ORI NET DEEPEST
	1057	33 56.150N	138 45.850E	76	G-17	ORI NET FINISH
	1200	33 46.770N	138 55.260E	1527		
	1218	33 45.250N	138 57.300E	1938	G-18	CTD-RMS START
	1237	33 45.660N	138 57.670E	1864	G-18	CTD-RMS DEEPEST
	1248	33 45.860N	138 57.810E	1834	G-18	CTD-RMS FINISH
	1254	33 45.960N	138 57.970E	1810	G-18	CHLTEC START
	1306	33 46.220N	138 58.280E	1785	G-18	CHLTEC FINISH
	1309	33 46.260N	138 58.450E	1769	G-18	ORI SIDE NET START
	1312	33 46.340N	138 58.680E	1747	G-18	ORI SIDE NET FINISH
	1318	33 46.430N	138 59.080E	1724	G-18	ORI NET START
	1331	33 46.650N	138 59.820E	1663	G-18	ORI NET FINISH
	1451	33 32.980N	139 09.150E	1927	G-19	XBT

Y.M.D	JST	LAT.	LONG.	DEPTH	ST.NO.	COMENT
	1554	33 21.920N	139 20.390E	1554	G-20	CTD-RMS START
	1614	33 21.970N	139 21.000E	1541	G-20	CTD-RMS DEEPEST
	1638	33 21.890N	139 21.250E	1536	G-20	CTD-RMS FINISH
	1642	33 21.860N	139 21.290E	1535	G-20	CHLTEC START
	1651	33 21.830N	139 21.450E	1568	G-20	CHLTEC FINISH
	1654	33 21.850N	139 21.440E	1570	G-20	ORI SIDE NET START
	1658	33 21.820N	139 21.380E	1529	G-20	ORI SIDE NET FINISH
	1704	33 21.750N	139 21.330E	1490	G-20	ORI NET START
	1714	33 21.740N	139 21.130E	1419	G-20	ORI NET DEEPEST
	1721	33 21.690N	139 21.020E	1384	G-20	ORI NET FINISH
	1800	33 26.120N	139 16.310E	2008		
	1913	33 38.740N	139 03.070E	1701	FN1-1	CTD START
	1922	33 38.920N	139 03.470E	1730	FN1-1	CTD DEEPEST
	1931	33 38.800N	139 03.670E	1734	FN1-1	CTD FINISH
	1937	33 38.930N	139 03.860E	1753	FN1-2	ORI NET START (60M)
	1941	33 39.050N	139 04.000E	1855	FN1-2	ORI NET DEEPEST
	1956	33 39.630N	139 04.600E	1840	FN1-2	ORI NET FINISH (60M)
	1958	33 39.680N	139 04.710E	1838	FN1-3	ORI NET START (120M)
	2004	33 39.910N	139 04.930E	1818	FN1-3	ORI NET DEEPEST
	2023	33 40.650N	139 05.740E	1825	FN1-3	ORI NET FINISH (120M)
	2027	33 40.800N	139 05.870E	1825	FN1-4	ORI NET START (180M)
	2033	33 41.000N	139 06.120E	1826	FN1-4	ORI NET DEEPEST (180M)
	2054	33 41.930N	139 06.940E	1828	FN1-4	ORI NET FINISH (180M)
	2057	33 42.010N	139 07.080E	1827	FN1-5	ORI NET START (200M)
	2106	33 42.490N	139 07.300E	1824	FN1-5	ORI NET DEEPEST (200M)
	2113	33 42.830N	139 07.440E	1813	FN1-5	ORI NET FINISH (200M)
	2158	33 37.570N	139 04.200E	1738	FNX	XBT
	2212	33 36.690N	139 05.640E	1875	FN2-1	CTD START
	2222	33 36.940N	139 06.020E	1862	FN2-1	CTD-RMS DEEPEST
	2228	33 37.090N	139 06.260E	1863	FN2-1	CTD FINISH
	2238	33 37.300N	139 06.710E	2259	FN2-2	ORI NET START (60M)
	2242	33 37.270N	139 06.720E	1861	FN2-2	ORI NET DEEPEST (60M)
	2256	33 37.380N	139 06.720E	1859	FN2-2	ORI NET FINISH (60M)
	2300	33 37.490N	139 06.720E	1858	FN2-3	ORI NET START (180M)
	2308	33 37.510N	139 06.710E	1857	FN2-4	ORI NET DEEPEST (180M)
	2328	33 37.720N	139 06.680E	1852	FN2-4	ORI NET FINISH (180M)
94.03.17	0000	33 39.470N	139 06.920E	1826		
	0400	33 52.460N	139 12.180E	4056		
	0800	33 54.920N	139 14.290E	1177		
	1200	34 31.040N	139 21.490E	281		
	1600	34 19.140N	139 20.030E	264		
	2000	34 28.010N	138 47.220E	564		
94.03.18	0000	34 14.420N	139 00.560E	665		
	0400	34 26.860N	138 44.950E	619		
	0403	34 26.840N	138 44.900E	620	G-21	CTD-RMS START
	0423	34 26.940N	138 44.840E	625	G-21	CTD-RMS DEEPEST

Y.M.D	JST	LAT.	LONG.	DEPTH	ST.NO.	COMENT
0436	34	27.070N	138 44.950E	612	G-21	CTD-RMS FINISH
0442	34	27.120N	138 44.920E	612	G-21	CHLTEC START
0449	34	27.160N	138 44.890E	611	G-21	CHLTEC FINISH
0454	34	27.260N	138 44.980E	615	G-21	ORI SIDE NET START
0455	34	27.290N	138 45.010E	607	G-21	ORI SIDE NET START
0501	34	27.430N	138 45.120E	592	G-21	ORI SIDE NET FINISH
0508	34	27.650N	138 45.350E	566	G-21	ORI NET START
0519	34	27.970N	138 45.600E	526	G-21	ORI NET DEEPEST
0524	34	28.100N	138 45.670E	516	G-21	ORI NET FINISH
0640	34	14.910N	138 56.050E	336	G-22	XBT
0748	34	02.860N	139 06.830E	729	G-23	CTD-RMS START
0808	34	02.780N	139 06.460E	775	G-23	CTD-RMS DEEPEST
0824	34	02.920N	139 06.270E	763	G-23	CTD-RMS FINISH
0826	34	02.940N	139 06.240E	756	G-23	CHLTEC START
0833	34	02.890N	139 06.100E	831	G-23	CHLTEC FINISH
0838	34	02.890N	139 06.030E	754	G-23	ORI SIDE NET START
0842	34	02.980N	139 06.030E	745	G-23	ORI SIDE NET FINISH
0846	34	03.100N	139 06.040E	739	G-23	ORI NET START
0857	34	03.390N	139 06.090E	719	G-23	ORI NET DEEPEST
0905	34	03.540N	139 06.040E	707	G-23	ORI NET FINISH
1017	33	51.080N	139 17.940E	1417	G-24	XBT
1123	33	39.270N	139 29.220E	1694	G-25	CTD-RMS START
1145	33	39.240N	139 29.880E	2201	G-25	CTD-RMS DEEPEST
1202	33	39.340N	139 30.470E	3007	G-25	CTD-RMS FINISH
1210	33	39.440N	139 30.520E	866	G-25	CHLTEC START
1219	33	39.690N	139 30.730E	1068	G-25	CHLTEC FINISH
1224	33	39.840N	139 30.980E	922	G-25	ORI SIDE NET START
1227	33	39.990N	139 31.210E	1318	G-25	ORI SIDE NET FINISH
1235	33	40.320N	139 31.720E	1513	G-25	ORI NET START
1246	33	40.850N	139 32.440E	1645	G-25	ORI NET DEEPEST
1255	33	41.260N	139 32.940E	1638	G-25	ORI NET FINISH
1426	33	41.980N	139 48.870E	1009	G-30	CTD-RMS START
1446	33	42.100N	139 49.190E	925	G-30	CTD-RMS DEEPEST
1456	33	42.210N	139 49.480E	872	G-30	CTD-RMS FINISH
1500	33	42.200N	139 49.580E	861	G-30	CHLTEC START
1508	33	42.280N	139 49.660E	838	G-30	CHLTEC FINISH
1600	33	50.240N	139 45.290E	1329		
1626	33	56.170N	139 41.850E	1106	G-29	XBT
1733	34	09.650N	139 35.570E	311	G-28	CTD-RMS DEEPEST
1733	34	09.650N	139 35.570E	308	G-28	CTD-RMS START
1747	34	09.470N	139 35.240E	237	G-28	CTD-RMS DEEPEST
1756	34	09.420N	139 35.100E	218	G-28	CTD-RMS FINISH
1800	34	09.370N	139 35.050E	224	G-28	CHLTEC START
1809	34	09.270N	139 34.870E	206	G-28	CHLTEC FINISH
1932	34	10.440N	139 34.890E	410	S-9	GILL NET IN
2149	34	10.470N	139 31.400E	167	S-9	GILL NET OUT

Y.M.D	JST	LAT.	LONG.	DEPTH	ST.NO.	COMENT
	2252	34 24.120N	139 28.880E	72	G-27	XBT
	2355	34 37.820N	139 23.070E	736	G-26	CTD-RMS START
94.03.19	0011	34 37.760N	139 23.120E	369	G-26	CTD-RMS DEEPEST
	0023	34 37.760N	139 23.210E	371	G-26	CTD-RMS FINISH
	0026	34 37.740N	139 23.210E	371	G-26	CHLTEC START
	0036	34 37.710N	139 23.270E	370	G-26	CHLTEC FINISH
	0043	34 37.600N	139 23.170E	371	G-26	ORI NET START
	0059	34 37.130N	139 22.830E	368	G-26	ORI NET FINISH
	0208	34 30.530N	139 23.700E	132	S-10	GILL NET IN
	0557	34 29.300N	139 22.190E	242	S-10	GILL NET OUT
	0800	34 32.100N	139 05.690E	504		
	1200	34 28.740N	138 37.160E	1683		
	1600	34 12.340N	138 59.910E	515		
	1817	34 19.660N	139 00.340E	403	S-11	GILL NET IN
	1948	34 19.370N	139 01.430E	152	S-11	GILL NET OUT
	2000	34 18.990N	139 00.850E	216		
	2053	34 19.930N	139 03.590E	230	S-12	GILL NET IN
	2243	34 19.320N	139 03.720E	208	S-12	GILL NET OUT
	2306	34 19.500N	139 03.990E	285	S-13	GILL NET IN
94.03.20	0000	34 19.430N	139 03.360E	188	S-13	
	0121	34 19.870N	139 03.450E	129	S-13	FINISHED GILL NET OUT
	0135	34 19.960N	139 03.360E	131	S-14	START GILL NET IN
	0153	34 19.940N	139 03.210E	144	S-14	GILL NET IN
	0259	34 20.440N	139 03.080E	116	S-14	START GILL NET OUT
	0317	34 20.530N	139 03.230E	76	S-14	FINISHED GILL NET OUT
	0330	34 20.580N	139 03.240E	133	S-13	CTD START
	0339	34 20.590N	139 03.240E	133	S-13	CTD DEEPEST
	0345	34 20.600N	139 03.230E	133	S-13	CTD FINISH
	0351	34 20.630N	139 03.270E	134	S-13	CHLTEC START
	0359	34 20.710N	139 03.290E	135	S-13	CHLTEC FINISH
	0400	34 20.710N	139 03.300E	135		
	0800	34 21.340N	139 02.370E	298		
	1029	34 48.440N	139 26.230E	911	KS-9	RELEASE FOR ADCP1
	1031	34 48.430N	139 26.200E	911	KS-9	POPPING UP OF ADCP1
	1101	34 48.460N	139 26.340E	873	KS-9	START TO RETREIVE OF ADCP1
	1118	34 48.450N	139 26.170E	840	KS-9	FINISH TO RETREIVE OF ADCP1
	1124	34 48.400N	139 26.200E	828	KS-9	CTD-RMS START
	1151	34 48.320N	139 26.260E	813	KS-9	CTD-RMS DEEPEST
	1201	34 48.220N	139 26.360E	789	KS-9	CTD-RMS FINISH
	1223	34 48.480N	139 26.290E	872	KS-9	MTD START TO TOWING
	1228	34 48.630N	139 26.350E	933	KS-9	MTD MESS CAST
	1237	34 48.820N	139 26.400E	1021	KS-9	MTD FINISH
	1551	34 19.890N	139 02.650E	127	C-1	START OF UNDERWATER TV
	1642	34 19.450N	139 02.830E	193	C-1	FINISH OF UNDERWATER TV
	1653	34 19.280N	139 02.880E	210	C-2	START OF UNDERWATER TV
	1724	34 19.030N	139 02.980E	252	C-2	FINISH OF UNDERWATER TV

Y.M.D	JST	LAT.	LONG.	DEPTH	ST.NO.	COMENT
	1736	34 18.890N	139 02.990E	313	S-15	GILL NET IN
	1853	34 18.420N	139 03.720E	595	S-15	START OF UNDERWATER TV
	1928	34 18.210N	139 04.090E	583	S-15	FINISH OF UNDERWATER TV
	1953	34 18.190N	139 04.390E	561	S-15	GILL NET OUT
94.03.21	0000	34 27.900N	140 19.550E	3186		
	0206	34 35.020N	140 22.400E	2965		PASSED K-90
	0247	34 40.010N	140 14.940E	2850		PASSED K-89
	0400	34 49.940N	140 00.020E	1753		a/co to 262°
	0800	35 00.150N	139 46.440E	343		
	0825	35 00.410N	139 47.920E	290		COMMENCED CALIBRATION
	0908	35 00.340N	139 47.660E	368		FINISHED CAL
	1300	35 34.010N	139 49.820E	124		LET'GO ANCHOR